Applications of Robotic Devices for Motor and Sensory Rehabilitation

by

Rhet O. Hailey

A thesis submitted to the Graduate Faculty of
Auburn University
in partial fulfillment of the
requirements for the Degree of
Master of Science

Auburn, Alabama
May 5, 2023

Keywords: Rehabilitation, Robotics, Assessment, Non-Pharmacological, Diabetic Peripheral
Neuropathy

Approved by

Chad G. Rose, Assistant Professor of Mechanical Engineering
Michael E. Zabala, Auburn Alumni Engineering Council Endowed Associate Professor of
Mechanical Engineering
Kristina A. Neely, Assistant Professor of Kinesiology

Abstract

With the increase of individuals effected by neurological disease, individualized rehabilitation methods can allow for improvement. Robotic intervention in rehabilitation enables a standardized, individualized practice that can allow for a higher dose of assistive care and intensity. This thesis focuses on robotic applications for rehabilitation by quantifying effectiveness of active gravity compensation in upper extremity exoskeletons alongside observing performance of nerve stimulation through a rehabilitation device. Gravity compensation in upper body rehabilitation has been used to delineate loss of strength and dexterity in spinal cord injury impairments. Through measuring and identifying movement quality, upper limb exercises can be improved for increased movement quality, which is focused on in Chapter 2. The exploration of a robotic device for a non-invasive pharmaceutical treatment is utilized to facilitate nerve sensation and growth along with increased blood-flow when neuropathy of the foot is present in Chapter 3. Robotic intervention offers a standardized approach to rehabilitation that can improve motor and sensory impairment.

Acknowledgments

I would like to express my gratitude and thanks to the following people. First and foremost, I would not have made it through this journey without my advisor Dr. Chad Rose for giving me the opportunity to work in the WeBR lab at Auburn University. Thank you to Dr. Michael Zabala and Dr. Kristina Neely for their time to help assist me as my committee members. Special thanks to my lab-mates Avinash and Chandler and the camaraderie and assistance they have provided. I would like to thank the RENEU lab at UT Austin for bestowing me with all of their motion capture knowledge. Thank you to Dr. Jon Commander and his assistance and help with the GAINS-Boot project in providing professional and anecdotal feedback on the device. Thank you to Dr. Tom Denney and his assistance with MRI bloodflow analysis. A special shout out is deserved to my friends from Mississippi State University and all the good times shared together. To my family, thank you so much for setting me up for a life of success and supporting me along the way. Thank you to my fiancé Ann who has kept me sane throughout this process.

Table of Contents

List of Tables

List of Abbreviations

ADL   Activities of Daily Living

COTS   Commercial Off The Shelf

DoF   Degrees of Freedom

DPN   Diabetic Peripheral Neuropathy

MRS   Modified Rankin Score

QoL   Quality of Life

RGC   Robotic Gravity Compensation

SCI   Spinal Cord Injury

SHR   Scapulo Humeral Rhythm

Chapter 1

Introduction

1.1 Background

More than 795,000 people suffer a stroke each year in the United States and are the leading cause of long term disability in approximately half of survivors with serious motor disability [7]. Globally, over 10 million people have strokes annually [8] Spinal Cord Injury (SCI) impacts around 17,000 every year with a total population of approximately 300,000 in the United States [9]. Average indirect additional costs for impaired individual are $77,000 providing added stress on top of disruption to Activities of Daily Living (ADL). Recovery is limited by damage to the corticospinal tract, with even strict therapeutic regimes to regain sensation being insufficient for total repair [10]. These injuries lead to muscle weakness and lack of fine motor movements. This creates a physical barrier for individuals that hinder ADL and may halt independence.

Diabetes is reported in 37.3 million people across the United States and can lead to peripheral or autonomic nerve damage with irreparable neurological impairment [11]. Peripheral neuropathy is quite common and affects a third of patients with diabetes in some capacity [11].

Damage to the nervous system will affect sensation, movement, and alter normal executions of ADL [12]. However, these damaged portions of the central and peripheral nervous system may contain pathways with the ability to regenerate sensation, or alternate pathways may be available.It is crucial to the impaired patient to immediately begin therapy within the first spontaneous recovery period of three months. It has been shown that the highest gains of recovery come during this plasticity period and show massive room for recovery gains [13]. Following the initial three month period, the average nerve damage has a band months wherein most typically functional recovery pathways can be expected but is not always the rule [14]. Sometimes, sensory and motor regeneration may continue long after initial damage.Nerve damage repair has multiple different intervention

1

methods that can be utilized such as: allografts, coaptation, and non-surgical approaches. These non-surgical approaches to nerve regeneration include pharmacological, electrical stimulation, and myelination recovery in order to promote therapeutic strategies to aid nerve growth [15]. These treatments combined with neurorehabilitation can allow for a maximum increase in neuroplasticity on the road to recovery.

Most rehabilitation today is still administered using traditional methods without access to a high enough dosage (number of practiced movements) and intensity (number of movements per unit time) [16, 17]. The number of repetitions, intensity, the amount of time spent, along with the effort it takes for a physical therapist or an assistant are some of the largest limitations surrounding these traditional therapy methods [18]. Another major factor in therapy methods is a standardized application in different therapies. While the methods themselves may be consistent across therapists, there proves to be a lack in exercise standardization that can be filled with precise, quantitative data from robotics. The application of robotic devices can allow for precise, repeatable training alongside doctors and physical therapists to allow for better treatments with higher intensity, dose, and precision. Robots have been proven to be safely implemented for multiple facets of rehabilitation through targeted device designs for any level of injury. Robotic exoskeletons for rehabilitation utilize unique system dynamics to provide various methods of movement that can be constrained and quantified to a range of parameters. This is important in the design and implementation of a device focused on rehabilitative gains to increase motor function. Unique, standardized metrics coupled with access to an high repetition without the need for therapist assistance increase the potential for improved rehabilitation outcomes.

1.2   Review of Robotic Exoskeletons in Rehabilitation

The individualized, highly repeatable and precise interventions that robotic devices are able to provide can potentially allow users to train and improve their functional outcomes.

1.2.1 Robotic Exoskeleton Origins

The idea of machines for rehabilitation began as early as the 1910s with Theodor Bündingen and his cyclical "movement cure apparatus" to assist in a stepping motion for patients with heart disease [?]. Designed to improve Quality of Life (QoL) , these devices naturally progressed with time, innovation, and the understanding of robotics. From guided motor devices, to bowden cable driven devices for joint therapy, and even onto pneumatic movement for joint control, the field of robotics has made large advancements alongside with the modern understanding of the body and machines [19]. Impedance control is an imperative factor in the kinematic manipulation of robotics, which allows for assumptions about position to be made alongside the force control to allow for a super-imposed implementation of control for a more accurate feel towards a true human movement dynamics [20].

1.2.2 Types of Robotic Exoskeletons

Traditionally, most rehabilitation robots can be classified into three separate types: grounded exoskeletons, grounded end-effector robots, and wearable exoskeletons [8]. Grounded exoskeletons connect in a serial manner to gain individual control of joints while remaining grounded at a base providing a mapping between joints to match the interactions between human and robot. This is different from grounded end-effector devices which give a higher range of motion-dynamics along with lower mechanical impedance and inertia with separate non-matching kinematics that still provide typical human range of motion. This allows for a greater control of end-effector impedance which can create the desired movement for therapeutic exercises. Wearable exoskeletons typically have some form of soft component such that the device remains compliant with true human range of motion. As this is an even newer facet of rehabilitation robotics, there is a much higher precedence for the realm of lower-extremity rehabilitation robotics with a focus on non-stationary movements to mobilize impaired individuals. As all of these design types have their own perks and drawbacks, it is important to keep in mind that each are designed for their own set of tasks.

1.2.3 Other Rehabilitative Robots

As one of the first true powered robotic end-effectors, the MIT-MANUS was developed and first implemented in 1992 specifically for stroke rehabilitation. The MIT-MANUS is a grounded end-effector uni-manual robotic arm that allows for planar manipulation of a single distal joint to help guide the entire limb [21, 22]. Through impedance control, the MIT-MANUS is able to work in a compliant operation with humans to remain safe without chance of injury and bring a standardized robotic method towards neuro-rehabilitation. The MIT-MANUS is not the only upper-extremity device created in the last 30 years; other upper-extremity robotic-devices exist such as the ARMEO Power, Kinarm, and Barrett [4, 23, 24].

The Armeo Power and Spring are unilateral, grounded exoskeletons known for offsetting user arm weight during patient interactions [25]. The Armeo Spring device is a 5-DoF orthotic robot with the same mechanical frame as the Armeo Power with the added benefits of remaining a truly passive device [4]. Three DoF comes from the shoulder with 1 DoF coming from both the elbow and the wrist. Typical use entails mimicking every day, functional tasks to be simulated in a virtual learning environment.

In rehabilitation robotics, most robotic exoskeletons are exclusively uni-manual robotic exoskeletons. However, there are a few bi-manual robotic exoskeletons that incorporate both arms into in the rehabilitation process. These robotic assistive devices typically use a mirror image movement of the arms to facilitate movement re-association in the neural pathways in hopes to help program growth throughout the damaged motor neurons. Through these mirrored, repetitive movements the aim is to focus on dominant motor movements to assist with ADL [26].

1.3 Harmony Exoskeleton

Harmony Exoskeleton [27] is a 14 (DoF) bi-manual upper extremity exoskeleton device centered on rehabilitation as seen in Fig. 1.1. The shoulder is supported with 5 DoF while the elbow and wrist each have a single DoF. With the provided force and impedance control capabilities, Harmony Exoskeleton allows for a large range of motion to allow each participant a more natural,

unhindered movement capabilities. A robotic exoskeleton attached around the user can benefit by providing mechanical assistance in given rehabilitative exercises.

Figure 1.1: Harmony exoskeleton, a bimanual, 14-DOF upper body exoskeleton provides gravity compensation of arm and exo weight during varied arm movements for participants with chronic stroke [1].

Stemming from the shoulder, the driving design behind Harmony Exoskeleton is to maintain shoulder dynamics and ensure proper scapulohumelar rhythm [28]. This proper design should allow for the setup of alternate linkages to allow for correct dynamics and kinematics. The shoulder is modeled in the Harmony Exoskeleton with 5 degrees of freedom to allow for free-use with minimal constraints. Both the elbow and the wrist are modeled with one degree of freedom each. As the elbow is properly one DoF, this allows for proper kinematics while the wrist only allows for pronation and supination.

1.3.1 Gravity Compensation

Gravity compensation is used extensively in the field of robotics and thus has extended out into the rehabilitative field for stroke therapy to allow for un-impeded movement dynamics of the

local extremities. The core identity between robotics and rehabilitation is the ability to manipulate known weights and countermasses to expand kinematic movement via gravity compensation tactics [29]. The objective is to remove the weight of gravity, which obscured potential functional abilities, through robotic interventions.

Removing the weight of the participant's arm reduces the strength requirement move, enabling more coordinated movements. Through these methods, underlying neural pathways can be excited to move their limb without being hindered by their own weight. Traditional methods use straps and pulleys from above the participant to be able to provide support which can be seen in Fig. 1.2 [2]. There are multiple other devices that are designed specifically to counteract gravity and are typically found in rehabilitation facilities targeted towards neurologically impaired patients such as the Swedish helparm, MIT-Manus, and the Armeo Power [2,4,30]. Robotic devices have been used to provide gravity compensation and are typically incorporated in their design framework. Such devices have different aims with varying degree of freedom. For example example, the ARMEO Spring can be utilized to help train the upper limb via a unilateral exoskeleton. The ARMEO Spring is 5 DoF with 3 in the shoulder with 1 each in the elbow and wrist and can allow for varying levels of gravity support [25]. Armeo has a powered robotic exoskeleton counterpart known as the Armeo Power that contains a powered gravity compensation component.

In summary, Harmony Exoskeleton provides a three-dimensional robotic workspace to implement rehabilitative tasks without being limited to two dimensions like some of the prior listed robots. Overall, with the use of all three dimensions, Harmony Exoskeleton provides an interesting insight into the world of robotic rehabilitation via measurement opportunities and task space.

1.4   Diabetic Foot Neuropathy Robotic Device Intervention

Robotic applications are not limited to rehabilitative exoskeletons and kinematic human movements. There are plenty of devices and deficits in the medical world that can be improved with automation of rehabilitative therapies such as virtual reality headsets and varying robotic arms to

Figure 1.2: The Freebal gravity compensation system (left) generates an upward force via inertia-free ideal-spring mechanism [2]. The Armeo Spring (Right) uses varied spring mechanism to help counteract the effect of gravity via gravity compensation [3, 4].

help aid in different tasks. Peripheral limb neuropathy is one such field that can be improved with the help of robotic device assistance for neural excitation and new, emerging therapies.

1.4.1 Peripheral Limb Neuropathy

Peripheral limb neuropathy is a common side effect of multiple diseases where feeling sensation is lost in the extremities and can be a cause of autoimmune diseases, varying violent infections, chemotherapy, and primarily diabetes [31]. Limb neuropathy is a result of damaged peripheral nerves causing weakness, numbness, and pain of the varying extremities. Neuropathy provides multiple difficulties for ADL. Specifically, diabetic peripheral neuropathy (DPN) is one of the most painful complications of diabetes. This pain can lead to injuries, falls, and even sepsis in particularly intense cases. If ignored, foot neuropathy can lead to foot ulcers, which can become inflamed and provide even more pain on the plantar surface. Extreme cases may lead to amputation of the lower limb. The most common treatment for limb neuropathy revolves around heavy pharmaceutical intervention and only treats the measurable symptoms of pain and inflammation as opposed to the cause of neuropathy itself [32]. As this short term relief may provide relaxation,

symptom treatment does not treat the root of the damage as this ailment will remain chronically present [32]. With minimal interventions showing efficacy in a non-pharmacological treatment, the opportunity for a robotic-treatment device arises to aid in a multi-factorial treatment approach.

1.4.2 Traditional Treatment Methods

Traditional treatment routes for diabetic peripheral neuropathy (DPN) are labeled as either pharmaceutical treatments or alternative medicine treatments. Primarily, symptoms of peripheral neuropathy are focused on more and as such are the primary focus of most treatment methods. This pain in the peripheral limbs is seen in upwards 30% of patients with DPN and is typically treated with tricyclic antidepressants, anticonvulsants, and serotonic-norepinephrine reuptake inhibitors, i.e. a pharmaceutical approach [33].

1.4.3 Non-Traditional Treatment Methods

Other non traditional methods of DPN exist including, but not exclusive to, therapies such as: whole-body-vibration, neurostimulation, vitamin D, meditation, and even yoga [32]. These varying methods may exhibit anecdotal results, but are not accompanied by much backing literature in the realm of DPN. Typically, these methods lead to a general, healthier lifestyle and improve QoL regardless of any ailments. In contrast, they are not inherently linked to any specific nerve healing and pain treatment of the peripheral nerves and exist as complementary and alternative treatment methods.

1.4.4 Robotic Non-pharmaceutical Treatment Method

Through the development of applied robotic intervention in therapeutic treatments to effected limbs, DPN can potentially be treated through robotic assisted rehabilitation therapy from a singular device. The goal behind such a device is to provide multiple stimuli to the injury site to help encourage for increased blood-flow to the effected area alongside nerve growth. The device design provided in this thesis is focused on a robotic boot device for a lower limb on a multi-factorial

approach to assistive treatment. Specifically, there are three main stimuli to be provided to the foot: heat, pressure, and vibration. Shown in Fig. 1.3, heat is provided in a uniform manner while pressure is provided in cyclical pattern starting at the base of the foot working its way up the leg. The vibration stimuli targets the distal phalanges, metatarsal heads of the foot, and following up the sural nerve.
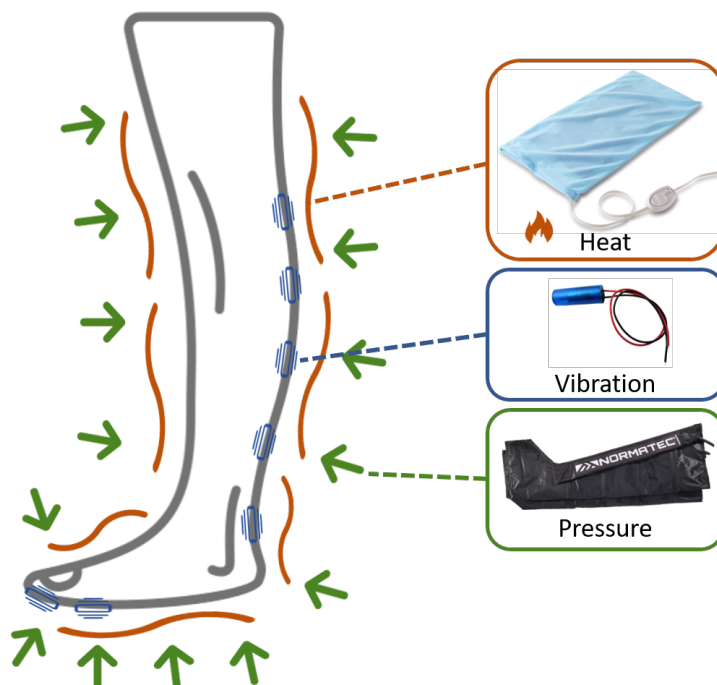
Figure 1.3: Diabetic Foot Neuropathy Treatment Boot Stimuli. In this figure, all three stimuli can be seen with their respective color: heat is outlined in orange, vibration in blue, and pressure in green.

1.4.5 Robotic Non-Pharmaceutical Application

In this robotic device, all three stimuli will be provided in controlled manner to provide a soothing, therapeutic, potentially efficacious sensation to the shank and foot. Both heat and pressure will be applied to the foot in a uniform manner being controlled to tolerable temperatures and pressure gradients respectively. The vibratory stimuli will target the distal phalanges and the metatarsals while also following the sural nerve up the back of the leg to promote nerve stimulation.

1.5   Robotic Interventions for Neurological Injury and Neural Conditions

With the widespread harm that neurological disease can have on the population, there is an ever growing need for motor and sensory nerve rehabilitation therapies and treatment. From complex upper-extremity exoskeletons to help focus on fine motor movements to lower body treatment modalities, applied robotics has a massive potential to help the impaired population gain back and help repair nerve damage. These treatment and therapy methods have been shown to help the impaired population by combining the worlds of rehabilitation and robotics.

1.6   Thesis Outline

This thesis is structured as follows: Chapter 2 provides insight into active gravity compensation use with the Harmony exoskeleton to explore varying assessment metrics of improvement for a chronic stroke population. Chapter 3 presents the device design for a non-pharmacological intervention for diabetic foot neuropathy via the application of robotic stimuli for motor and sensory improvement. Chapter 4 outlines a pilot study to validate and implement the device design from the prior chapter. In Chapter 5, I will conclude the findings of this thesis.

Chapter 2

Gravity Compensation in Upper Extremity Exoskeleton Movements

2.1 Introduction

Individuals affected by stroke and other injuries may suffer extreme upper extremity impairment which can be attributed to a lack of strength, dexterity, and coordination [34]. Depending on the severity of stroke, side effects may range from short term impairment, to an injury that persists throughout the remainder of life. The after effects of a stroke vary greatly from person to person and require individual-based therapy to help improve sensorimotor function. Typically performed by physical therapists and their assistants, therapy programs can take weeks of individual 1-on-1 sessions that can be very labor intensive and time consuming. Most traditional therapies include resistance training and repetition of traditional movement exercises to help recover movements to restore activities required in every day life. Other therapies and training might include resistance training, weight training, or even spring and cable machines such as the Freebal or other gym equipment [2].

Traditional training methods for gross upper and lower extremity movements in an impaired population involve weight offloading in order to promote free motion. This allows for neural pathways that may be previously obscured by the effort required to lift and move one's own body weight. Therefore, by counteracting the weight of gravity with cable pulleys and exoskeletons, gravity compensation leads to a path of recovery for the impaired patient population. An individual's body weight and mass may hinder movement if the neural pathways are too severely damaged and may cause issues when attempting to overcome the inertia provided by body mass.

I hypothesize that the with the removal of a strength requirement from the gravity compensation, that rehabilitation of dexterous movements will improve movement quality. [1]

In particular, studies in chronic stroke populations which use robotic devices such as Harmony Exoskeleton (Fig. 1.1) to create or mediate experimental conditions [35] can be valuable for investigations into new therapeutic interventions or the fundamental neuromuscular function behind stroke impairment [19]. Studies in chronic stroke populations, despite limitations in potential motor recovery, can be valuable for investigations into the relationship between the neuromuscular control strategies available to individuals after a stroke for motions that require strength and/or precision. [36]. By utilizing the large population with chronic stroke, upper extremity exoskeleton rehabilitation intervention can continue expanding rehabilitation methods and movement learning towards recovery and improvement. [19].

A primary interest in this thesis is the relationship between neuromuscular control strategies available to an impaired, post-stroke individuals for both strength and dexterity. It has been shown that reducing upper extremity torque requirements through gravity compensation of limb weight can reveal motor function otherwise obscured by weakness or abnormal joint coordination patterns [37]. Previous studies have suggested that the partial loss of corticospinal pathways leads to increased reliance on remaining neural pathways, resulting in abnormal coordinations and reductions in workspace [13, 36, 38]. When strength output requirements are high, the body may rely on less coordinated pathways to perform tasks as a maladaptive strategy caused by a focus on task completion (and away from movement quality) [36]. As shoulder torque output requirements increase, abnormal joint coordination patterns between the joints of the upper extremity increase, reducing workspace [37]. Similar coordinations have also been seen in isometric joint torque generation tasks [39]. Offloading limb weight, via Robotic Gravity Compensation (RGC), can allow for improved performance and control [40], seen as increased range of motion, accuracy, and potentially improved movement quality, as measured by various smoothness metrics [41].

---

[1]Portions of this chapter originally appear in a paper submitted by Hailey, de Oliveira, Ghonasgi, Deshpande, and Rose [1]. Here, this work was expanded to include additional presentation of results and discussion.

2.1.1 Gravity Compensation

Gravity compensation is an exercise tactic utilized to aid in the discovery of old and new neural pathways to improve kinetic movement. Through the use of exercise machines and robotics, body weight may be offset to help remove any bodily resistance provided from the force of gravity which allows for a "free-form" like movement of the body. This improved performance can take the form of increased range of motion, accuracy, and improved movement quality, as measured by smoothness metrics. Robotic exoskeletons are a promising platform for research into these interventions and assessments.

The MIT-MANUS, first introduced in 1992, was one of the first and most influential modern upper-extremity exoskeletons in teaching therapies for both mind and hand manipulation which forces these two factors to communicate in tandem [30]. With the novel concept of providing a multi-sensory experience, the MIT-MANUS was designed to help facilitate motor skills towards an impaired population with 5 DoF from a 5 bar linkages to relate to a planar motion for the participant [30]. The MIT-MANUS operates via impedance control which has been shown to guarantee passivitiy through control and interaction of the dynamic environments [20]. Since its conception, the MIT-MANUS has shown great improvements to the severely, chronically impaired population with an improvement of 10% over its 12-week programs [42]. One thing to note, however, is that the length of therapy interventions is crucial towards seeing improvements in functional outcomes. At a minimum, the duration of the rehabilitation should last 6 weeks with 5 trials per week [36, 42].

Another primary example of an upper extremity uni-manual exoskeleton is the ABLE from Garrec *et. al* [43]. This platform was created with a multi-purpose use case in mind to be utilized in traditional clinics, virtual reality, impaired patient assistance and tele-robotics as a haptic device. The ABLE Exoskeleton uses screw cable system (SCS) actuators for joint and torque manipulation. Using position control to help counteract the weight applied by gravity, the ABLE exoskeleton focuses on a positional system to help generate the required forces needed to complete a given task.

The T-WREX exoskeleton is a passive uni-lateral exoskeleton with 2 DoF at both the shoulder and the the elbow [44]. As a predecessor to the Armeo Spring, the T-WREX primarily offsets the weight of gravity to help the user complete rehabilitative exercises by mimicking a weightless infrastructure providing a perfect balance for the wearer. Apart from powered robotic exoskeletons, passive exoskeletons allow for an added layer of comfort and added safety net for the patient that the T-WREX and Armeo Spring bring. In terms of recovery and improvement, the T-WREX showed similar return values on the Fugl-Meyer assessment to other active end-effector, such as the MIT-Manus [3, 44].

2.1.2 Harmony Exoskeleton

The Harmony Exoskeleton is a bi-manual upper-extremity exoskeleton with 14 DoF, 7 for each arm. The shoulder girdle represents 5 DoF with the other DoFs at the elbow and wrist respectively. It has both position and torque control capabilities with the series elastic actuators enabling high performance and impedance control [20, 28]. Prior results from de Oliveira *et al.* [39] suggested that the coordinated movement training was beneficial, showing anecdotal evidence through improved FM-UE and ARAT scores. Additionally of interest from this previous study were the maladaptive muscle coordination patterns seen in isometric force generation tasks, which suggests that these patterns may be a limiting factor in upper extremity function for the pilot study participants. With this in mind, understanding the impact of gravity compensation, a common method for reducing this discoordination, could lead to improved intervention design.

Harmony Exoskeleton uses a multi-level control structure to maximize both performance and safety. At the lowest level, the Harmony Exoskeleton uses a joint-level torque measurement for controlling each of the seven DoF of the arm (elevation-depression and protraction-retraction of the shoulder girdle; abduction-adduction, flexion-extension of the elbow; and pronation-supination of the forearm) [1]. This torque control has a bandwidth of 7 Hz, which is within the desired range of typical human motion. Also within normal ranges of motion, typical speeds from impaired

participants are less than .5 m/s with a few peaks less than .7 m/s as can be seen with an example oscillatory motion in the Harmony Exoskeleton in Fig. 2.1.
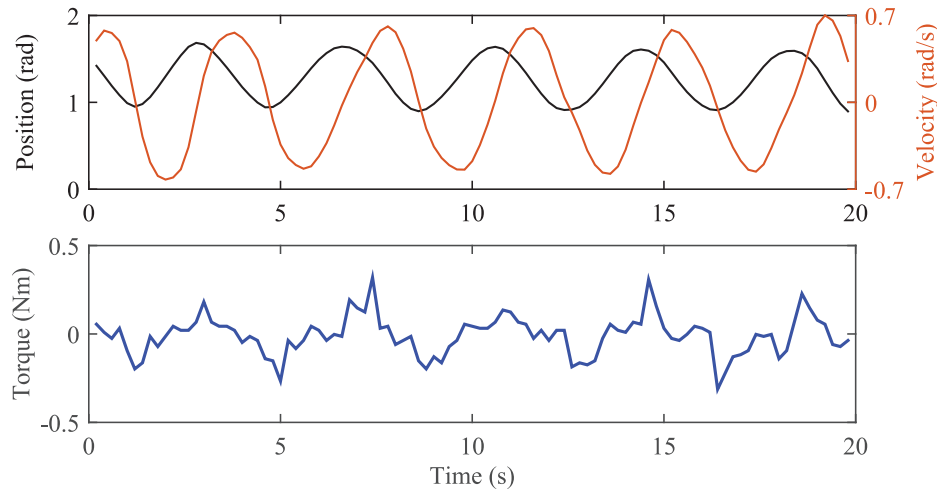
Figure 2.1: Shown above is typical position and velocity data of a participant wearing Harmony Exoskeleton. Both position and velocity are shown in rad and rad/s respectively. Shown below is a sample of torque output for the joints.Typical Harmony speeds remain below .5m/s while no torque needed should be above .5 Nm allowing for smooth, subtle movements to be able to wear and control the Harmony Exoskeleton.

Containing a feed-forward control, Harmony Exoskeleton diminishes friction and viscous damping of the joints which result in a resistive torque of .2 Nm at max velocities present from this study. This can be seen in the following diagram in Fig. 2.2. Following this torque control, the Harmony Exoskeleton implements gravity compensation utilizing the weight of the wearer to maintain an accurate SHR. Specifically, an inverse dynamics algorithm containing forward and backward kinematic recursion calculates and implements compensatory torques [1].

In RGC mode, arm weight of the participant and the robot are offset to allow for a free-floating experience. With the control inactive, in the NGC mode, the robot gravity compensation is passive and only allocates for the weight of the exoskeleton. During NGC mode, the dynamic model of the wearer is turned off while the robot remains active which allows for the series elastic actuator's naturally low impedance to encourage voluntary movements. The resistive forces applied at the interactive points were in a range of ± 2.5N, which can be seen in Fig. 2.3. This allows for low effort
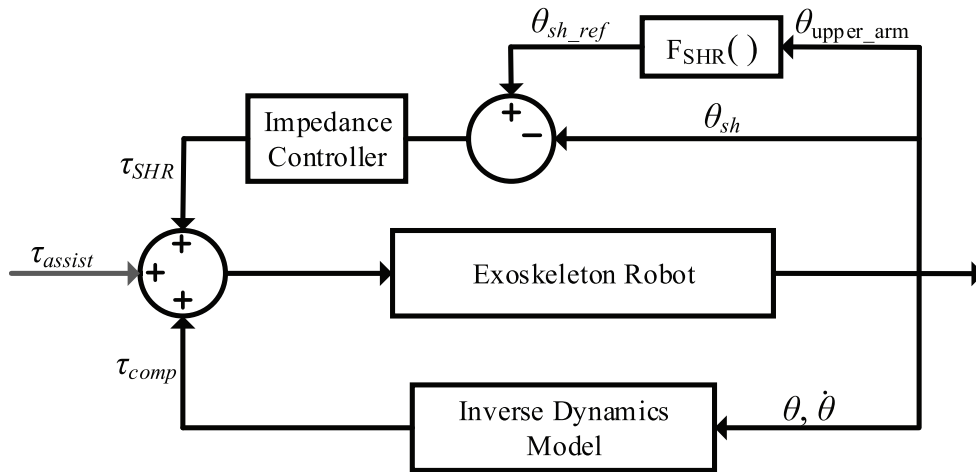
Figure 2.2: Harmony exoskeleton requires a foreknowledge of the user's upper limb length. This data was recorded and implemented into the kinematic model during the screening process for each participant and then utilized in the following block diagram for sufficient torque control.

movement from the participant to maintain a passive movement whilst wearing the exoskeleton. During the initial setup phase, each participant was fine tuned using their measurements and dimensions to correctly alter the dynamics model per each individual before any robotic movements took place.

2.2 Experiment Design

Utilizing these gravity compensation methods, a study was designed with a chronically impaired patient population with the goal to investigate changes in movement quality in gravity compensated reaching and coordination movements. For this experiment, each participant was enrolled in seven one hour sessions with two per week with a pre- and post-assessment session attached as well. These sessions incorporated passive and active stretching sessions on top of gravity compensatory robotic therapy session with multiple exercises using varied levels of complexity. These exercises are broken up by section and are described as they appear in this thesis. During these training sessions, the only feedback provided to each participant was verbal feedback from the on-sight occupational therapist and any kinesthetic feedback from Harmony Exoskeleton during

16
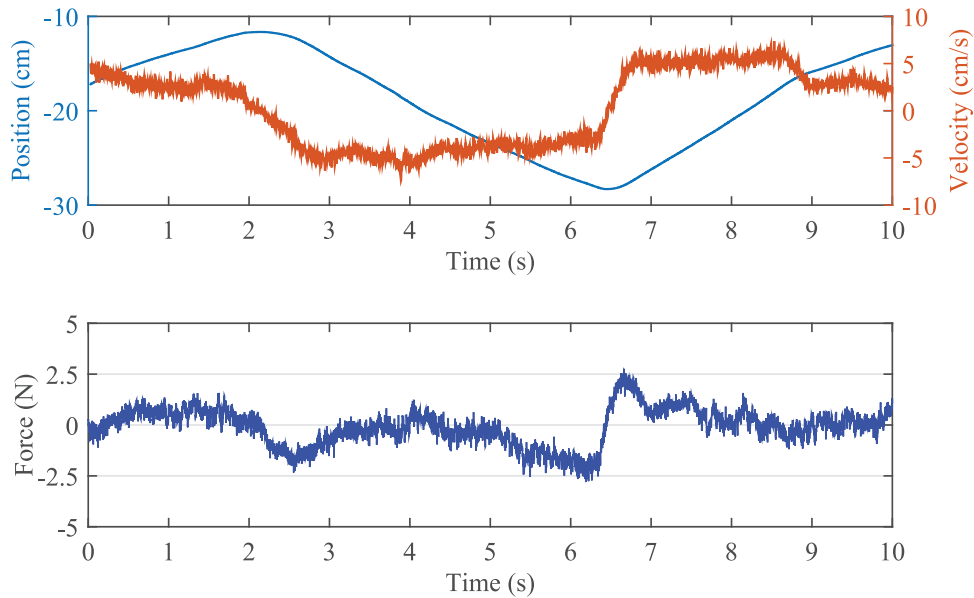
Figure 2.3: During the No Gravity Compensation mode, the individual effort remains low with less than ± 2.5 N of Force needed to overcome any stiction or resistivity provided by the exoskeleton. After overcoming any stiction phase, Harmony exoskeleton should see the active movement to enable the participant to move freely. Overall, this allows for individual effort to remain low with slower than normal movements.

motion. All of these movement tasks were designed to focus on singular DOFs or multi-joint motions with varying levels of complexity, mentioned at each intervention. Every participant in this study completed over 1000 repetitions throughout this pilot study.

Primary analyses comes from the post-assessment data to ensure a non-bias towards any 'learning' of how to use Harmony Exoskeleton. Fig. 2.4 is an overall view of the combined reaching and coordination data to demonstrate that movements of each participant did get smoother overall suggesting improvement over this brief pilot study. With a mean increase in both metrics of SPARC from the assessment tasks, improvement can be inferred as SPARC values closer to 0 represent more efficient movements. Fig. 2.4 shows the most improvement with the robotic gravity compensation active for both reaching and coordination.
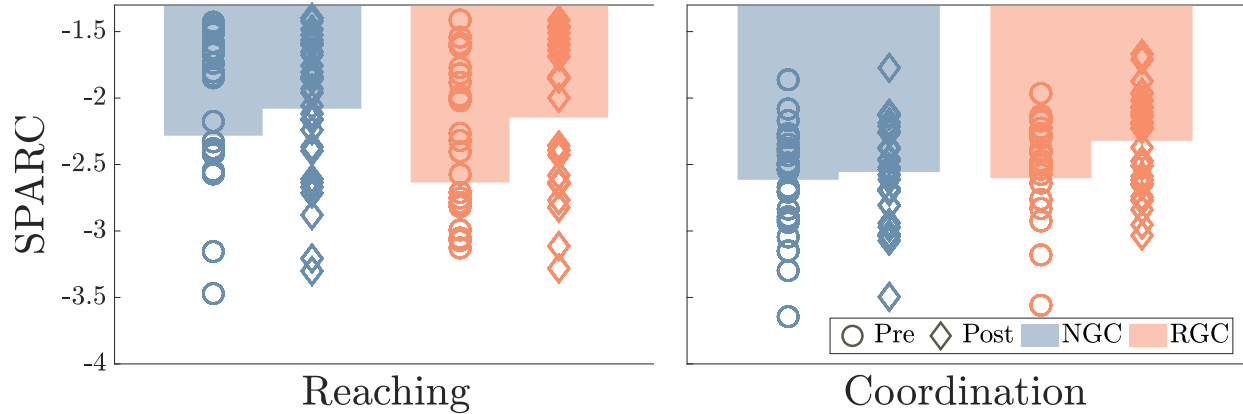
Figure 2.4: Pre and Post assessment of movement quality (SPARC) separated by condition (robot gravity compensation (RGC) and no gravity compensation (NGC)) and task (reaching/coordination). Increase in reaching (All targets) and coordination tasks (SR, SE, and ID combined) in the gravity compensation condition could suggest improvements in performance due to training.

2.2.1 Participants

For this study, the participant population were individuals with chronic stroke and with a Modified Rankin Score (MRS) of less than or equal to four [45]. Of the six participants recruited for this study, participant 3 did not meet the inclusion-exclusion criteria. Participants 5 and 6 are at the forefront of most of the data due to their being the most and least impaired participants. Participant information can be shown below in Table 2.1 for the most and least impaired participants.

Table 2.1: Demographic data of participants

	S5	S6
Age	55	63
Months post onset	30	10
Mod. Rankin Score	2	2
Affected/Dominant Side	L/R	L/R
Post-Study [39] FM-UE Score (Δ)	24 (+10)	49 (-2)

2.2.2 Metrics

All movements were captured via a 10-camera optical motion capture system (Optitrack Prime 17W system, NaturalPoint Inc., Corvallis, OR, USA) at 80 Hz. Point trajectories of the motion capture points in Motive:Body were manually checked for labeling errors and point corrections

for the fluidity of marker movement for each of the tasks. To reduce noise in marker position, a low pass Butterworth filter with a cutoff of 6 Hz was applied minimally for error correction native inside Motive:Body software mostly used on missed data points. Kinematic data for the reaching task was segmented with a 5% velocity threshold for separation of different reaching movements. Post processing included a fifth order Savitzky-Golay filter with 21-sample window added for all marker positions before analyzing and quantifying movement positions and velocities [46].
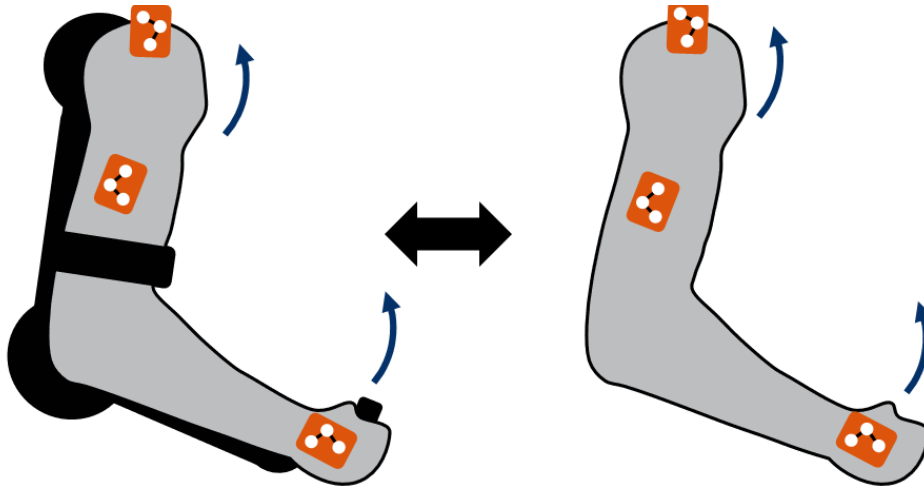
Figure 2.5: Shown above is an diagram of marker placement in the RGC(left) and the NGC(right) conditions. Markers were placed in the same orientation at the same bony landmarks on each individual for any condition.

Several metrics have been suggested to assess and compare performance changes due to rehabilitation [41,47]. To determine movement quality, in this manuscript I focus on two measures, an established metric spectral arc length (SPARC) and a quantification of the deviation from the most efficient straight line path in Cartesian space, similar to previously presented measures [46,48]. In reaching, the maximum distance from the initial point by a straight line integrated against the absolute value of the movement path was defined as straight line deviation (SLD):

$$\textbf{SLD} = \int_0^{t_f} \frac{(|X_{pos}(t) - X_{SL}|)}{\|X_{SL}\|} dt.$$

With SLD, the closer the value to the origin, the lower the deviation from the most efficient path which infers that values closer to zero are the most optimized path

Using the MATLAB function and default settings from Balasubramanian [49], Spectral Arc Length (SPARC) extends on Spectral Arc Length Measure (SAL) with retained sensitivity, and is utilized to quantify movement quality through smoothness

$$\text{SAL} \triangleq -\int_0^{\omega_c}\left[\left(\frac{1}{\omega_c}\right) + \left(\frac{d\hat{V}(\omega)}{d\omega}\right)^2\right]^{\frac{1}{2}}d\omega$$

where

$$\hat{V}(\omega) = \frac{V(\omega)}{V(0)}$$

with the caveat for SPARC that the cutoff frequency ω_c is chosen from the spectrum of the relative velocity profile.

$$\omega_c \triangleq min\{\omega_c^{max}, min\{\omega, \hat{V}(r) < \bar{V} \forall r > \omega\}\}\ (5)$$

SPARC, as outlined by Balasubramanian *et. al* [49], estimates the arc length of the Fourier magnitude spectrum within 0 to 20 Hz of a speed profile where any value closer to 0 returns a more "smooth" value.

2.2.3   Task Description

There are two sets of separate tasks outlined throughout this study: reaching and coordinated movement tasks. For the reaching task shown in Fig. 2.6, three targets were placed in a straight line directly in front of the participant wearing the exoskeleton at a distance of 75% of maximum reaching distance with each participant being able to reach the central target with their wrist [50]. These targets were placed in plane, ipsilateral, and contralateral to the impaired participants shoulder. The ipsilateral and contralateral targets were placed 10 inches away from the center target in their respective directions. The target's height was controlled per participant to be in plane with the shoulder such that the shoulder and target are in plane when the elbow is flexed 90°. These participants were then guided in a pseudo-random order to reach for each target 5 times while Harmony exoskeleton is in a passive state. This was followed with the exact same scenario in a new pseudo-random order with RGC active with an optional rest period in between sessions to reduce possibility of fatigue. I hypothesized that changes in workspace brought on by increased shoulder abduction torque requirements would also affect movement quality.

20

Figure 2.6: Reaching targets were set up in a line in front of the seated participant at elbow height (left) and set at a distance requiring 75% of reachable distance (right). Three targets were presented in the task for the participant: ipsilateral (orange), contralateral (purple), and the center target aligned with the shoulder (green).

In the coordinated movements task, each participant performed sets of three repetitive movements, again in a pseudo-randomized manner, in order to study the effect of gravity compensation in an impaired population. There were two modes with varying aid from the Harmony Exoskeleton, (NGC) and (RGC). These three movements can be seen in Fig. 2.7. The shoulder rotation

Shoulder Rotation   Scapular Elevation   Inward Diagonal

Figure 2.7: Participants performed a set of six coordinated motions during training, and in this thesis we analyze the impact of gravity compensation on a subset of three movements, which involve different levels of effort and shoulder coordination. Specifically, shoulder rotation, scapular elevation, and across-the-body inward diagonal motion.

movement incorporates the medial rotation of the shoulder while the elbow remains 90° in a natural resting position. Scapular elevation requires the elbow to remain at 90° angle while the shoulder

flexes 90°, raising the arm and hand above the shoulder and ideally the cranium. The inward diagonal incorporates both of these motions in tandem to raise the arm from rest to medially rotate the humerus and flexing the shoulder in tandem to reach across the body in an 'inward diagonal' motion. These movements were demonstrated to each participant prior to evaluation by the attending occupational therapist. This task provided no visual feedback, with the only feedback modality being the prior demonstrations. Listed from least to most complex, these tasks have differing ranges of gravity compensation active. The shoulder rotation task rotates mostly around the plane perpendicular to gravity. Scapular elevation adds gravity as a complexity while remaining a one degree of freedom movement while also introducing the need for some strength and SHR coordination. However, the inward diagonal takes both of these movements and combines their complexities into one fluid motion with the most complex joint coordination pattern of these coordinated movements.

2.3   Results

In the post-study assessment of the reaching task (Fig. 2.11), gravity compensation provided by Harmony Exoskeleton resulted in an increased smoothness for the most impaired participant (S5) and a reduction in smoothness for the least impaired (S6). This follows previous results [37, 39] which suggests that impairment may result in an over-reliance on sub-optimal neural pathways. While it is possible that the reduction in smoothness for S6 was due to a robot-imposed reduction in compensatory strategies, the minimal changes in SLD (Fig. 2.11) and lack of trunk movement (Fig. 2.8) suggest other causes. Each participant was strapped into the Harmony exoskeleton and was instructed not to move their torso. However to ensure that there were no compensatory strategies of the body, local trunk movement was compared with hand trajectories to ensure that there was no change from the data based on any movement from the participant as can be seen in Fig. 2.9.

In the coordinated movements, S5 and S6 improved in their SPARC values across all three tasks with the exception of the scapular elevation task, where S5 had a slight downward trend
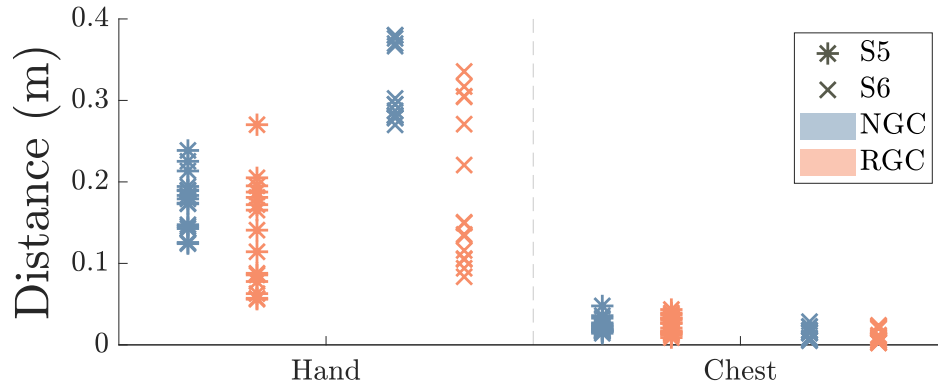
Figure 2.8: Motion of the hand and the chest was examined to determine if compensatory strategies contributed to differences in movement quality between robot gravity compensation (RGC) and no gravity compensation (NGC) conditions. Maximum distance of the hand (left) and the chest (right) suggests compensation strategies were minor.

(Fig. 2.10). Each task required varying levels of shoulder torques to overcome gravity, along with differing levels of joint coordination.

Improvement of motor impairment has been seen before from de Oliveria *et al.* when comparing FM-UE and ARAT scores as indications of stroke recovery [39]. From de Oliveira *et al.*, both metrics increased showing positive results with minimal significance, all due to low dosage of rehabilitation intervention. However, reaching showed a positive, upward trend for S5 (most impaired) and a negative, downward trend for S6 (least impaired) as shown in Fig. 2.10.

This result might suggest that a higher impairment leads to larger improvement capabilities as opposed to a lower impairment which leads to less improvement possibilities. However, these opposing results in SPARC values between the robot and no-robot condition for S5 and S6 and ultimately leave with mixed results of movement smoothness. SLD (Fig. 2.11) for these tasks reveal same result with S5 with improvement in deviation from the no-robot to robot condition while S6 showed minimal to no change. This was true for all targets with no variation. Different compensation strategies were possible as to why results for the reaching task differed from the expected outcome. Trunk displacement from the initial position was considered and seen to be a factor for some participants. Maximum hand distance from initial differed for each participant, where ROM may be a limiting factor. However, hand distance relative to chest position was investigated to
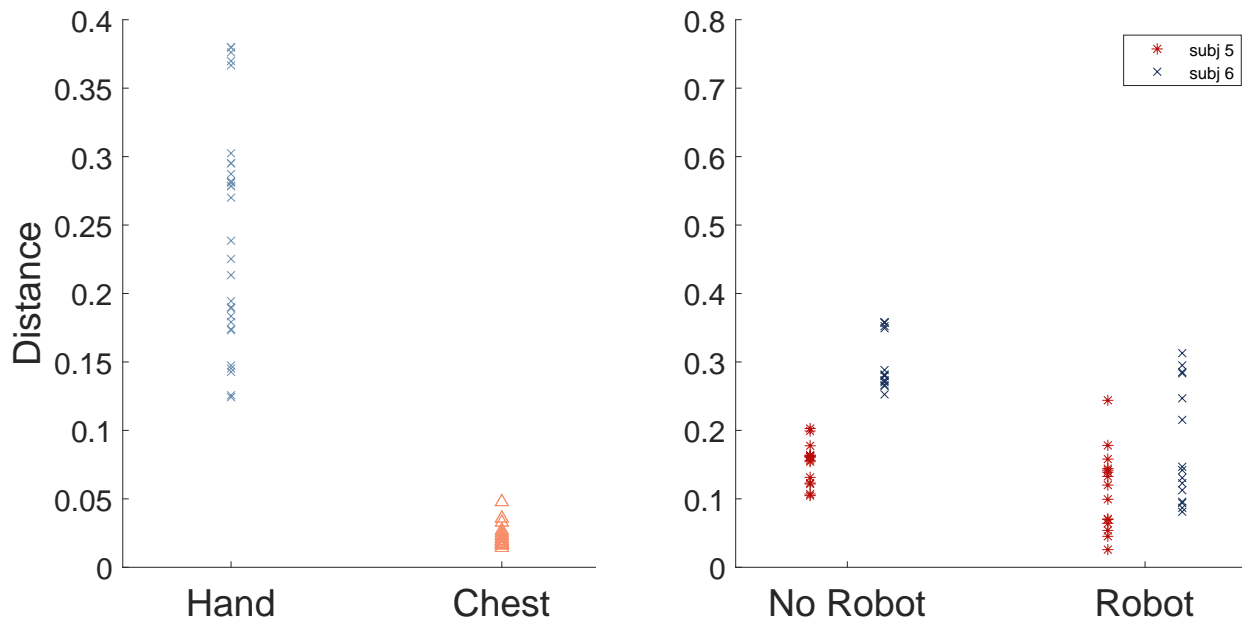
Figure 2.9: Hand reaching distance for all 4 combined participants in this study (left) and the hand distance relative to the chest displacement (right). From this figure, it is possible to see that the average spread of the hand relative to the chest looks even across the Robot and No-Robot categories, which suggest minimal compensation strategies.
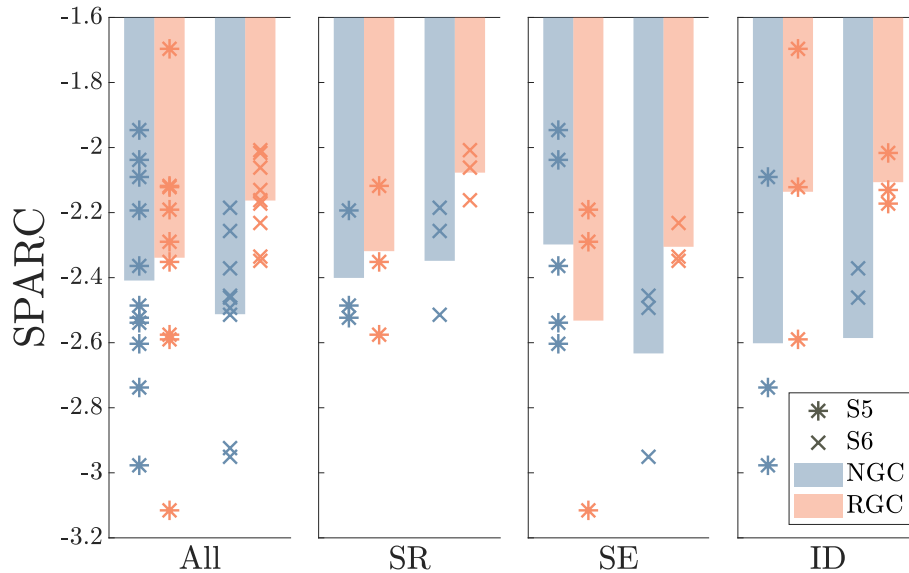
Figure 2.10: Movement smoothness (SPARC) of three different coordinated tasks: Shoulder Rotation (SR), Scapular Elevation (SE), Inward Diagonal (ID) motions separated by participant and condition. For the simplest (SR) and most difficult (ID) motion, gravity compensation increased smoothness, with mixed results for scapular elevation(SE).

normalize the averages hand displacement difference that trunk movement might play on reaching of which there were no observable difference between the robot/no-robot condition for S5 and S6.

Unpaired t-tests were performed to compare robotic gravity compensation and no compensation for both the reaching and coordination tasks per each individual movement. The coordinated tasks were shown to be statistically significant between the RGC and the NGC categories for the coordinated moving tasks as $0.010 < \alpha$. For the reaching tasks and the difference between participant 5 and 6, the differences in the categories were not shown to be statistically significant. The data can be shown in Table 2.2. This might be the result of analyzing only two participants and with more participants, a clearer separation between these cases would show more significance.

Table 2.2: Unpaired t-test for movement smoothness

	t-statistic	p-value	df
Coordination RGC/NGC	-2.66	0.010	74
Reaching RGC/NGC	1.101	0.276	58
S5/S6	-1.23	0.219	134

Overall, the most impaired participant (S5) showed the highest potential for an increase in movement smoothness and improvement under the influence of gravity compensation. The FM-UE scores for the participants are shown in Table 2.1. The averaged movement smoothness (SPARC) values are summed up into Table 2.3 and show that each participant is showing an overall smooth movement where a normal movement smoothness of an unimpaired person is around -2 to -1.5. Overall, both participants show improvement wearing the robotic exoskeleton.

Table 2.3: Movement smoothness per target

	No-Robot	Robot
All	-2.03 ± 0.71	-2.15 ± 0.72
Ipsilateral	-2.10 ± 0.63	-2.12 ± 0.52
In-Plane	-1.84 ± 0.38	-2.17 ± 0.59
Contralateral	-2.14 ± 0.99	-2.18 ± 0.99
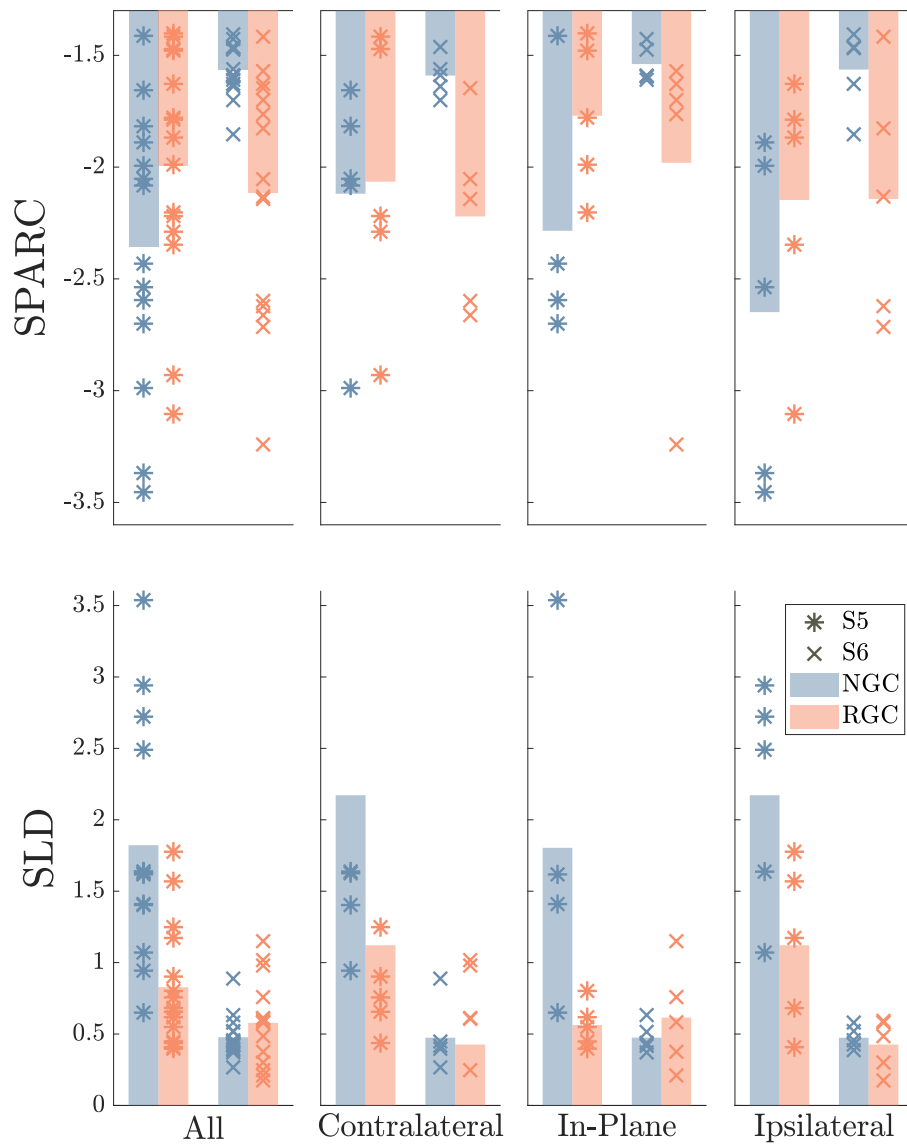
Figure 2.11: Movement quality for S5 and S6 in the reaching task. Top: Movement smoothness (SPARC) for reaching tasks separated by target and participant condition (robot gravity compensation (RGC) and no gravity compensation (NGC)). SPARC was calculated on hand trajectories in Cartesian space, suggesting that in general, NGC conditions were smoother for the less impaired participant (S6) and comparable for the most impaired participant (S5). Bottom: (SLD) for reaching tasks separated by target, condition (RGC/NGC), and participant. SLD was calculated on hand trajectories in Cartesian space, with similar results to movement smoothness, where participant S6's change was minimal, and S5 saw a reduction in curvature.

2.4 Discussion

In Fig. 2.11, S5 is shown to have a complete across the board improvement in both SLD and SPARC in the reaching task. This means that not only did S5 take a more optimized path for each of the targets whilst wearing the assistive robot, but that the movements were more smooth and that the robot was able to assist more, since more assistance was needed for the greater impaired participant. However, S6 almost had an opposite trend. S6 was less smooth while wearing Harmony Exoskeleton in the reaching task, but effectively took same amount of optimized path whilst wearing the robot.

Another interpretation as why S6 showed no minimal to no change between RGC and NGC would be that Harmony exoskeleton and gravity compensation perturbed the motion of S6, either due to control strategy or kinematic overconstraint, which might have provided minuscule elasticity between the robot and human joints [51]. Gravity compensation, as implemented in this study, is not able to completely remove the dynamic impact of the friction and inertia inherent to the robot, potentially adding some mechanical filtering or disturbances. However, the joint-level torque control performance and high backdrivability [27] due to the low impedance from the series elastic actuators, combined with the relatively slow speeds at which the participants moved in this study reduces the impact of both friction and robot inertia. The increases in smoothness in the shoulder rotation coordination task for both participants (Fig. 2.10) suggests that the limitations of the gravity compensation implementation did not perturb motion. The task-oriented nature of reaching may be the cause of this reduction in smoothness. Visual feedback, coupled with the reduction in effort due to gravity compensation might have enabled additional, corrective motions to improve target reaching accuracy at the cost of movement smoothness. Also, it is possible that only participants with low levels of impairment could make these additional corrective motions.

By focusing on the coordinated motions without any visual feedback, the most important quality of the task turns toward the task itself instead of reaching an end goal which may lead to a more prominent method of improvement of movement quality [52]. By focusing on quality of movement, there may be potential to uncover and re-tune finer motor movements as opposed to

having to focus on directly achieving the task. There were two factors which may have resulted in gravity compensation causing greater changes during the coordination movements than in the reaching tasks.

First, when comparing the reaching and coordination tasks, the movement quality in differing levels of 'refinement in participants' internal models must be considered. Realizing functional improvements or changes in movement quality may be easier in novel coordination tasks than familiar reaching tasks. In contrast, the coordinated movement which had no target or quantitative value to reach but only qualitative motion completeness allows for better movement quality in the coordination task seen in Fig. 2.11. As can be seen from the pre-post assessment in Fig. 2.10, this focus on movement quality and smoothness, instead of correctness or a finite target, allows for a larger gain in movement improvement. This is similar in concept to as discussed by Krakauer [36] with neuroanimation therapy, which allows for more focus on movement quality instead of completing a set, defined task.

Second, improvements in movement quality seen across pre- and post-study assessments (Fig. 2.4), may not be the sole result of experience with Harmony. These improvements may be the result of achieved gains in function [39] and suggest further potential room for gains. By eliminating instantaneous visual and kinesthetic feedback, these movements tasked subjects to focus on learning the motion itself. This learning goal may result in a more effective improvement of movement quality [36], as opposed to the completion and accuracy focus of the reaching task.

2.5 Limitations

However, this pilot study has some limitation which may impact the clarity of results. Changes in feedback modality (visual vs. none) varied between task type and condition, potentially limiting the comparison of reaching and coordination tasks.

The differences between the tasks and the relative gravitational effort required by Harmony exoskeleton may contribute to the differences in result for reaching and coordination tasks. The reaching task, even with the ipsilateral and contralateral targets, required less shoulder torque than

some of the coordinated tasks (SR), which might potentially complicate interpretations of task orientation vs. exploratory movements. Lastly, a small sample size prevents a robust analysis for confirmation of this hypothesis. However, anecdotal evidence is supported by prior work utilizing gravity compensated training and suggests directions for future study.

2.6 Future Work

The differences seen between task-oriented reaching motions and quality-focused coordination support further investigation into gravity-compensated upper-extremity rehabilitation interventions. The changing landscape between task-oriented motion verses quality supported motion raise excellent questions and exploration into the world of neurological rehabilitation. Based on the anecdotal results outlined by this thesis and [1], the continuing study will revolve around constant user feedback along with varying tweaks in the assisted therapy methods that Harmony Exoskeleton may provide. The next study building on these anecdotal results should seek to further explore the effects of feedback and increased training focus on movement quality over task completion without changes in feedback modality. Our next investigative study will be formed around gravity control with consistent feedback levels and new improvements and tweaks for assisted therapy methods. Movement perturbations on coordinated movements [45, 46] may also provide improved metrics of kinematics and dynamics to better quantify and attribute the role of the exoskeleton onto the participant.

2.7 Conclusion

Movement quality style results can help aid neural pathways associated with dexterous human control via gravity compensation. These results from movement quality focused training, instead of task completion or strength motivated studies, can target neural pathways associated with dexterous control and can be aided by gravity compensation. These results may favor improvement over task completion or strength oriented tasks for improvement of movement quality. Utilizing these different task modalities can allow for a multi-tiered approach to improvement for ADL.

Here, I sought to determine affects of gravity compensation on the movement quality of reaching and coordinated movement tasks. We hypothesized that these movements would show improvements in quality for both participants with chronic stroke enrolled in the study. However, gravity compensation seemed to matter less, in particular for the less impaired participant, for the planar reaching tasks than the coordinated movements. These results, while anecdotal, motivate further study to better understand the role feedback and the focus on task completion or movement quality play on the restoration of motor function.

Chapter 3

Non-Pharmacological Peripheral Neuropathy Boot Treatment Device

3.1 Introduction

Peripheral neuropathy can be painful and affects the lives of an ever increasing number of individuals every year. Peripheral neuropathy is an often common side effect of patients with type 2 diabetes but is also associated with direct nerve damage, chronic liver or kidney disease, and various types of cancer [32]. 60% of diabetics will develop peripheral neuropathy [11]. As outlined in the introductory chapter, the beginning treatments for patients with peripheral neuropathy are typically pharmaceutic agents targeted towards treating pain symptoms, but these interventions do not treat the root cause of the symptoms. Pharmacological treatments may also lead to non-intended symptoms from these potentially harmful drugs that are typically prescribed.

I propose a non-pharmaceutical garment-based device that allows for an non-invasive approach to a therapeutic treatment that address the underlying mechanisms causing neuropathy [53]. Currently, there are no devices that can apply a cyclic pressure gradient, controlled heat therapy, and vibrotactile stimulation directly to the sural nerve and metacarpals. There are other devices marketed for athletic recovery such as the Aquilo unit and the Rapid Reboot Unit [54, 55]. However, these devices are limited in their delivery of stimulation and do not allow for a cyclic pressure gradient as they only have one chamber. Additionally, the lack of focused devices is compounded from a lack of clinical research to motivate their design and typically rely on anecdotal motivation for their device creation inspiration.

To close this gap of lack of clinical research, I have implemented a logical approach of utilizing mechanical systems to treat diabetic peripheral neuropathy through the use of the Garment Application of Intelligent Non-invasive Stimulation Boot (GAINS-Boot) to apply three stimuli to the foot. This garment applies a tri-modal stimulus applied to the leg and shank: heat, pressure,

and vibrotactile stimulation. Heat has been known to improve cardiovascular function and increase vascularization of the arteries [56]. Applied heat can decrease vascularization resistance and may point towards long term benefits in the reduction of resting blood pressure [56]. By applying heat directly to the foot, physical ailment from both diabetes and peripheral neuropathy may be facilitated towards a healing process. With the improvement of vascularization from the heat therapy, the hope is to encourage the removal of peripheral edema coupled with a simultaneous pressure therapy.

Compression therapy has been shown to be quite beneficial to aid patients impaired by poor blood circulation, or to help rapidly recover for any muscle soreness; compression therapy is very common amongst athletes after particularly difficult training sessions to help decrease swelling. Leg oedema, swelling caused from a build up of fluids, is a common side effect of patients with diabetes that can also provide pain [57]. Pressure therapy through the use of a intermittent pneumatic compression (IPC) has been shown to aid circulatory conditions [58]. Vibrational stimulus is an ever growing therapy sensation that has been used to help stimulate nerve endings. From Takatsura *et. al*, vibrotactile stimulation helped stimulate neuronal activity through vibrational motors at 140 Hz [59]. From this study, I aim to help encourage neural stimulation in the foot via the garment to help encourage nerve pain reduction in peripheral neuropathy [60]. By peering into a undeveloped field of non-pharmaceutical intervention of DPN, I aim to explore a robotic device application towards treating DPN in an inexpensive, portable manner.

This device was the direct inspiration for the Neuropathy Cartographer shown in Fig. 3.1 [61]. Of which, the driving purpose behind the Neuropathy Cartographer is to standardize and provide a numerical analysis of the sensation on the plantar side of the foot. Through the removal of human bias, a robotic test-bed can apply a Semmes-Weinstein monofilament directly to the bed of the foot to reduce inconsistencies between physicians and to interpret foot pressure sensation distribution more evenly. The devices tests multiple, physician chosen, targets across the surface of the foot testing at different forces to help determine sensitivity of the skin receptors [14]. This Neuropathy Cartographer device motivated the GAINS-Boot in order to standardize monofilament

measurements across medicine in order to analyze performance foot skin receptors and of any future device, i.e. the GAINS-Boot.
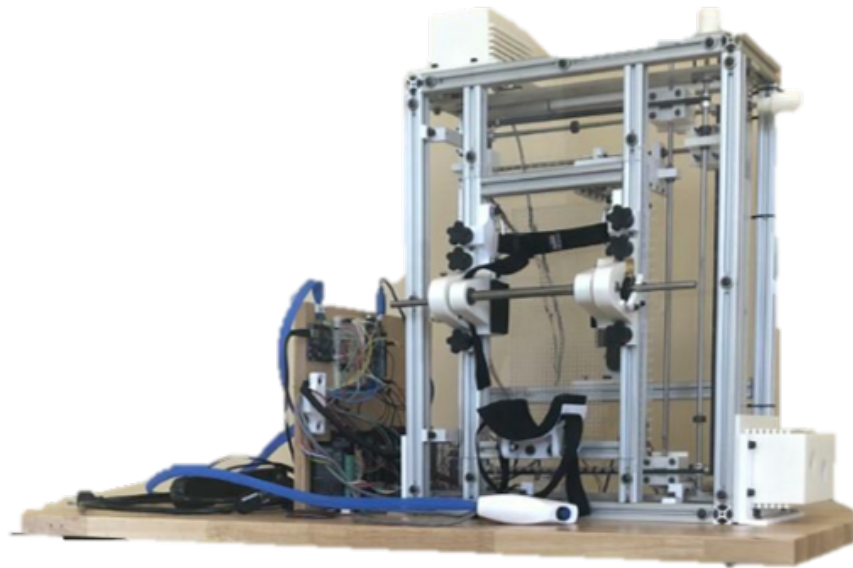
Figure 3.1: Neuropathy Cartographer testbed device which utilizes a standardized monofilament assessment procedure [5]. This device operates by moving the monofilament to designated targets along the sole of the foot before testing foot pressure sensitivity to assess foot neuropathy impairment levels.

3.1.1 Device Proposal

The GAINS-Boot is split up into three subsystems offering controlled heat, pressure, and vibrational sensations. As can be seen from early proposal images in Fig. 3.2, each mechanism is aimed to be applied evenly across the foot and shank.

The Boot Design presented by Castellano is shown in Fig. 3.2 with a heated water pump design [61]. Through a series of of one way valves and solenoids, a water pump with controlled water temperature was proposed to provide a heated, pressurized boot design targeted towards a population with foot neuropathy, seen in Fig. 3.2. However, this device could be applicable to any population with acute foot pains to sooth discomfort [5].

3.1.2 Continuation

In the next phase of the boot design, major key implementations were changed to fit a tighter timeline with a quick turnaround. Unlike the proposed water pressure valve, an array of squeeze bands was proposed to simplify the complications that hydraulic pressure provide. This was thought to reduce price, while increasing customizability, modularity, and greater flexibility. In turn, this changes the heating mechanism which was altered to be provided from resistive heating elements which allow for a uniform heating according to given material properties. Lastly, a new stimulus component was added by introducing multiple different vibrotactors to add multiple zones with separate vibrational sensations.

Through the introduction of a closed loop temperature, pressure, and vibrational controls, this device can be automated to run through the applied sensations over a given time period which can be pre-determined by an sight medical doctor or therapist. The temperature control was to

(a) Initial Design

(b) Secondary Design
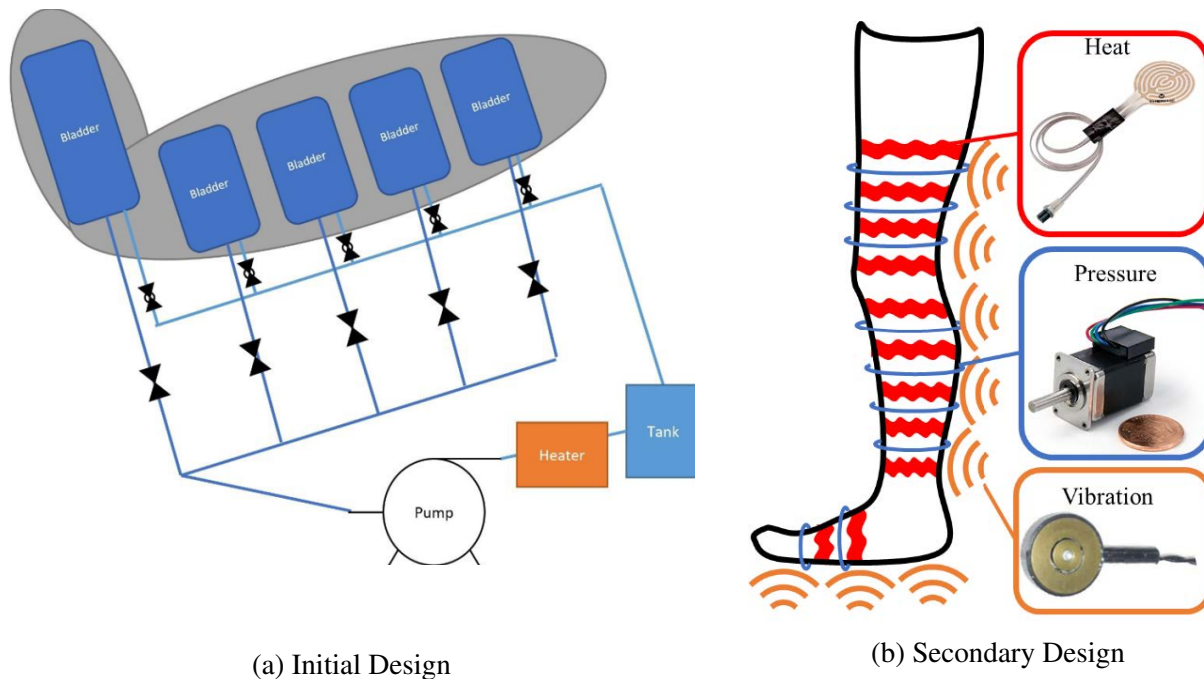
Figure 3.2: Proposed diabetic foot neuropathy boot treatment device (left). In this phase of the device, the boot would have a water-chamber system with heat controlled water to be pumped in increasing temperature to provide a heated, controlled pressure gradient. Newly proposed device design incorporating heat, pressure, and vibration stimuli to treat underlying causes of DPN in a uniform, guided manner (right).

be set to 100°F within 1°F, pressure to be controlled to 50 mmHg within 5 mmHg at a 1/10 Hz refresh rate, and 5 distinguishable vibrational stimuli to 5 different zones throughout the foot and shank. Following the creation of the device and validation with healthy participants, this device will be implemented in a clinical studies trial with non-neuropathic diabetic and neuropathic diabetic patients.

(a) DC Motor   (b) Heating Pad   (c) Vibrotactor

Figure 3.3: Different Commercial off the Shelf Items used for the GAINS-Boot testbed device for DPN.
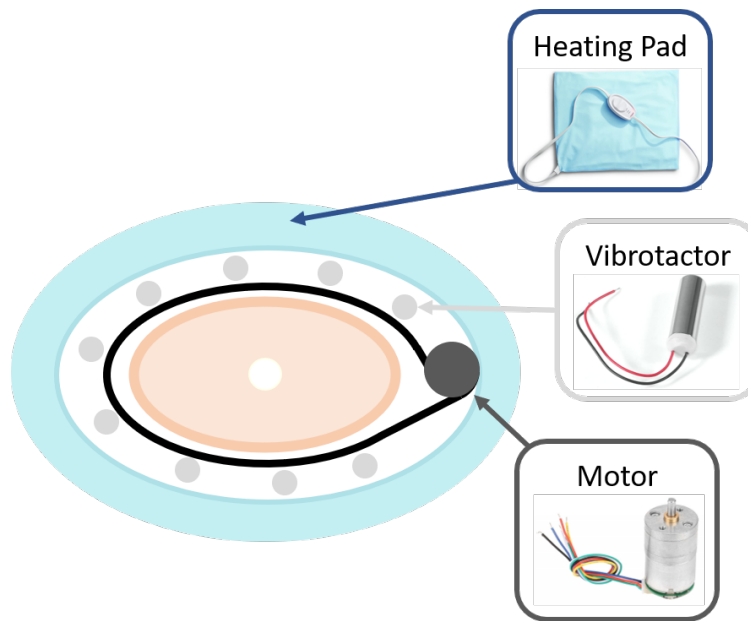
Figure 3.4: Proposed GAINS-Boot cross section of all three stimuli with heat (light blue), vibro-tactor array (silver), and motorized pressure strap(black).

The commercial off the shelf (COTS) materials of this iteration of the GAINS-Boot can be seen in Fig. 3.3. A cross section of the leg, shown in Fig. 3.4, shows a typical distribution of all of

the components on the leg. The DC motor was outfitted with a mounting mechanism along with a spool and strap in order to apply a pressure sensation across the surface of the shank and foot, which can be seen in Fig. 3.4 and 3.5. The original idea was to use this strap with vibrational motors attached around them with an even distribution to be able to determine multiple haptic schedules with the idea to aid nerve stimulation throughout the peripheral limb. All of this was to be covered by COTS heating pads to help regulate device internal temperature for a heating sensation to help reduce oedema and promote an increased blood-flow to the foot allowing for a net outward flow of oedema.

(a) Strap Visualization

(b) Strap Example

Figure 3.5: GAINS-Boot pressure, haptic strap sensation proof of concept utilizing DC motors (left) and the squeeze strap implementation (right).

Multiple iterations of a haptic strap were evaluated and tested in order to combine variability to haptic, pressure sensations along with a different feel to each one of them. Some of these iterations are shown in Fig. 3.5 along with multiple proposed ideas for this pressure sensation. Ultimately, this idea was passed down to be able to utilize a pneumatic pressure boot, Fig. 3.10, to provide a uniform pressure over the entire lower limb. This move from providing force over an area with DC motors to a pneumatic garment allowed for a much cleaner control of the pressure being applied with a pressure sensor in the feedback loop, along with a significantly more uniform

distribution of the pressure provided over the leg. This garment from Normatec utilizes 5 separate chambers to help apply pressure across the entire shank and foot [6].

Vibrotactile stimulus was originally supposed to be supported along with the haptic pressure straps to be able to provide vibrational patterns to the foot. After the decision to move away from DC motors, the vibrotactors needed to moved throughout garment in order to apply vibration stimuli cleanly to the entire leg. Shown below in Fig. 3.6, this was a separate strap that was to be utilized inside of pneumatic boot to continue on with customizable placement locations on the leg. This was then to be repeated up the leg in an equidistant manner.

For the temperature control of the boot, an example of multiple heating pads can be shown on the right in Fig. 3.6. This allows for equal heating by closing the feedback loop with high resolution thermistors for a temperature reading.

A.) Pneumatic Compression
B.) Heating Pad
C.) Vibrotactor Sleeve

(a) Vibratory Strap Example

(b) Stimuli modules

Figure 3.6: On the left is an example of the strap attached around the leg inside of the pneumatic compression boot. GAINS-Boot example stimuli testbed device. This image shows a concept of all three stimuli, labeled above, across the entirety of the shank and foot(right).

3.2 Final Design

With the culmination of the pneumatic pressure, closed loop temperature, and the targeted vibrotactile stimulation, the GAINS-Boot device aims to help treat DPN and help soothe other ailments of the lower leg and foot area. This non-pharmacological device will be used to execute a validation pilot study in aims to help uncover improvement through the therapies provided by GAINS-Boot. The final design sub-system can be seen in Fig. 3.7 with uniform pressure and heat while the vibrotactors attached at specific, targeted locations. The established device can be seen closed up and inflated in Fig. 3.11 to exemplify the GAINS-Boot looks in use.
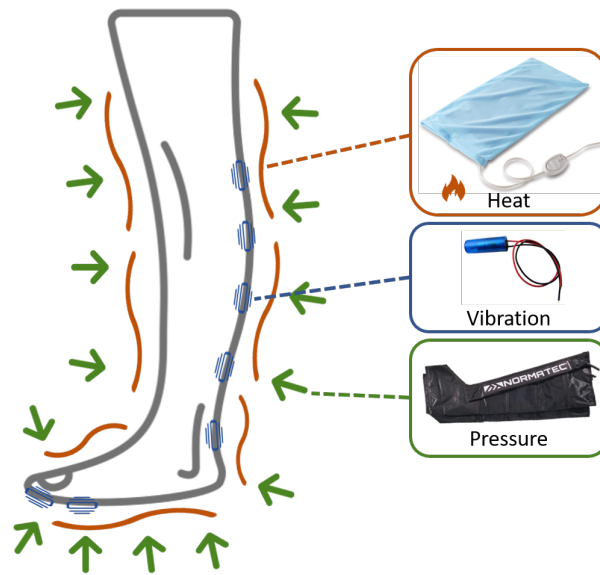
Figure 3.7: GAINS-Boot testbed final design. Shown above, both heat and pressure, orange and green respectively, are applied in a uniform manner to the foot and shank. The vibratory stimulus, blue, is applied to each of the distal phalanges? and metacarpals on the foot before following up the sural nerve on the backside of the shank.

3.2.1 Heating Elements

The heating element provided by GAINS-Boot comes from an array of multiple COTS heating pads that are ready available. These heating pads allowed for a clean, safe implementation that would not overheat the leg to excess and cause burns. For the temperature control of the heating pads, they were commanded via an AC relay switch at 1 Hz. with thermistor sensors readings
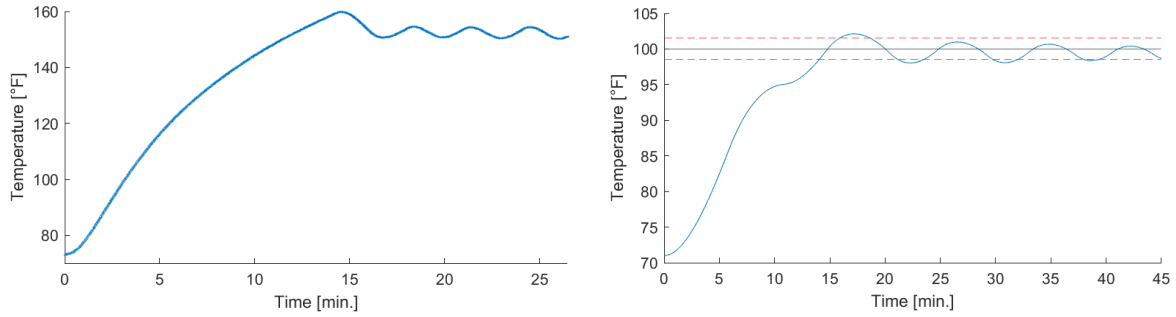
Figure 3.8: Extra Large Sunbeam heating pad step response: uncontrolled (left), controlled (right). The beginning room temperature was shown to be 74 F with an oscillatory steady state value of 152 F. This system simulation was then modeled and controlled using a model predictive look ahead distance to keep the temperature steady at 100°F within the bounds of 1°F.

every 10 Hz [62]. All digital readings were filtered with a Butterworth filter at a cutoff of 10 Hz to ensure no sensor noise could pass through. With a time constant around 6 minutes, 1 Hz control was used to control the internal garment temperature to 100 degF with a variability of 1 degF as can be seen in 3.8.

3.2.2   Vibrotactile Stimulation

Before, the vibrotactors were to be placed equidistant surrounding the leg for the most potential customization to haptic scheduling to help promote nerve stimulation. However, the vibrotactor array was redesigned to target simulation of the metacarpals, distal phalanges, and sural nerve, with motors at the physical location along the nerve path. Five motors were connected to two straps that could wrap around the metacarpal heads and distal phalanges with a 3D printed motor holder per each motor which was then threaded into a velcro attachment strap which is shown in Fig. 3.9. This allows for maximum adjustability to ensure that the locations be primed and corrected for any participant or wearer of the GAINS-Boot device. The other six vibrotactors were attached up the back of the boot following the sural nerve.

Each motor utilizes pulse width modulation to provide a maximum voltage of 3.3 volts sent to the motor with a maximum amperage of 0.2 amps. Each motor is connected via a 0.2 A fuse to a power-bank that is stepped down from the wall to 3.3V with a large fuse that does not allow for more than 5A distributed over 16 motors per each individual boot from GAINS-Boot. Images of

(a) Target Vibratory Stimulus   (b) Vibratory Stimulus Implementation
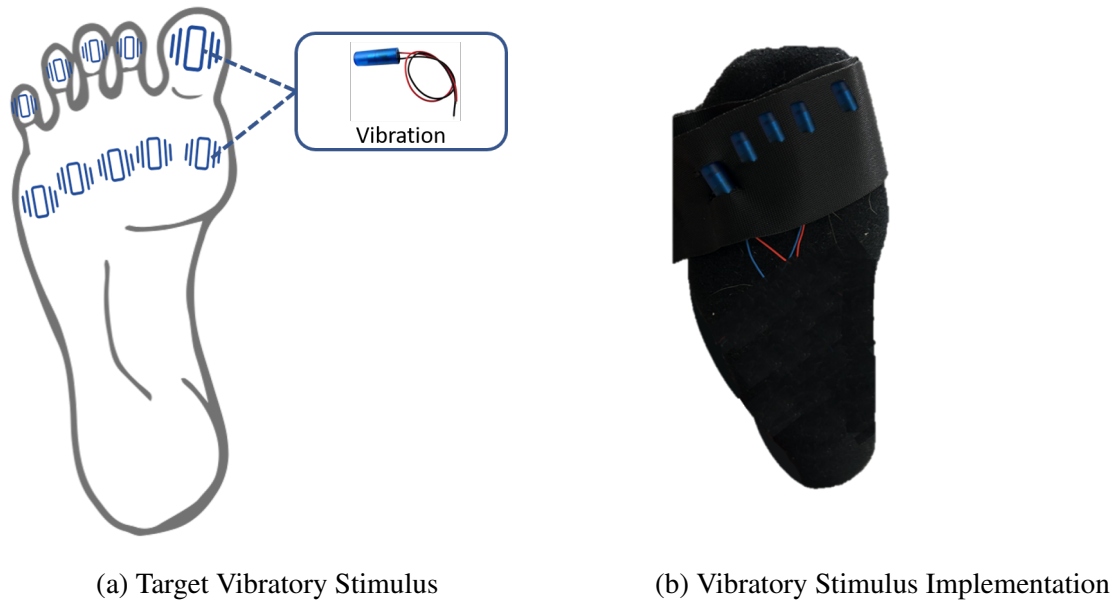
Figure 3.9: Shown above is the targeted stimuli location for the vibratory stimulus on the foot (left) and the implementation (right). The five distal phalanges and five metacarpals are shown above on the foot. The strap implementation, right, shows the vibrotactors attached only to the distal phalanges.

the circuit diagram for this design can be shown in Appendix A along with the micro-controllers used.

3.2.3 Pressure

The pressure sub-system was executed from the COTS boot, Fig. 3.10, from the Normatec company with a typical pressure of 50 mmHg [6]. These boots utilize pneumatic pressure to multiple chambers over the leg and shank over the course of a 45 minute therapy session. The desired pressure could be altered mid-session in order to ensure that participants were never uncomfortable or needed to stop mid session.

3.2.4 Programming Implementation

All self controller sub-systems were controlled and implemented in either C++ or circuit-python via a RP2040 Raspberry Pi pico. For the temperature control, each individual heating pad had its own feedback loop through thermistors that were read in through I^2C and each was

Figure 3.10: Normatec pneumatic boots targeted and marketed towards athlete for post-workout recovery [6].

controlled by a relay for an adjustable control law. The vibrotactors were controlled via pulse-width-modulation using transistors to simulate a lower powered motor driver for vibrational and magnitude control. These motors were also controlled and scheduled from a RP2040, one per each boot. The code for both subsystems can be found in Appendix A.

PCBs were created for each RP2040 to help execute the desired circuit design efficiently. Circuits for both the temperature control and the vibrotactile stimulation control were needed, designed, and utilized in this device design. Each of the RP2040s were connected over serial to a Raspberry Pi 4 to publish control data via ROS2 for data-logging purposes. Both the circuitry designs as well as all device implemented code may be found in Appendix A.

3.3 Conclusion

In summary, the GAINS-Boot uses a tri-modal system to apply a controlled temperature, pressure, and vibrotactile stimulation to the participant in aim to help abet PPN or any other peripheral limb neurological diseases. Future work includes implementing this non-pharmacological garment

Figure 3.11: Closed boot from GAINS-Boot aided by velcro straps to help keep the compressive garment closed with an even distribution of controlled pressure for participants.

in a pilot study to validate a potential road to recovery through this therapeutic device. As seen in Fig. 3.7, both heat and pressure are applied to the leg in a uniform manner while the vibration is placed in a precise manner. A preview of the GAINS-Boot can be seen in Fig. 3.11 where all subsystems are active.

Chapter 4

Garment Application of Intelligent Non-invasive Stimulation Boot Preliminary Validation

4.1   Introduction

The long-term objective of this pilot study is to develop a non-pharmacological intervention garment to help improve QoL in a diabetic population with DPN. By pursuing a non-pharmacological approach, disruptive drugs may cause long term effects or alter pain tolerance may be bypassed to still pursue treatment for PPN. This garment is based on the biological processes behind DPN and provides thermogenic, compressive, and vibrational stimuli to target vascular supply degradation to nerve fibers from a buildup of peripheral edema. This work will build upon prior work developing wearable devices for rehabilitation by creating a novel foot sensation diagnostic tool that quantifies foot sensation at an order of magnitude higher resolution that the standard clinical method [5].

4.2   Experiment Design

There are two groups present in the feasibility study: diabetic patients without signs of DPN or diabetic patients with signs of diabetic DPN. Before and after each intervention period, the participants will have the soles of their feet tested via the neuropathy cartographer and a MRI scan to determine bloodflow in the ankle before and after therapy. All participants will describe their day to day pain using traditional metrics such as the Defense and Veterans Pain Rating Scale (DVPRS). During the study, the participants will be listened to and periodically asked to verify comfort levels. Each intervention session lasted 2 weeks with 10 total session with each session lasting 45 minutes with a planned donning and doffing time period of 15 minutes. In actuality, the donning and doffing time should be fairly minimal as the GAINS-Boot is simple and easy to

put on. Any participants with competing vascularization diseases are disqualified, and will not be considered for the study.

Pre-study baseline measurements will be compared to post-study measurements in order to establish healing improvement and beneficial effects. This will provide a variance for the power analysis to help guide the design of future studies. Included in these measurements, an MRI will be taken of the participants ankle to calculate and plot bloodflow to see if there is any improvement post treatment.

4.3   Assessment Metrics

All MRI bloodflow measurements were taken with a 3 Tesla coil phase contrast MRI (PC-MRI) machine. The PC-MRI allows for the measurement of vessel size and flow rates. All bloodflow data was analyzed from the flow analysis software CV Flow (Version 3.2). Semi-autonomous contour was utilized to determine the various artery regions of interest in the magnitude and phase plots [63]. From this data, the velocity and bloodflow data was analyzed using MATLAB to compare pre-intervention data to post-treatment results. Along with these sets of data, a qualitative pre- and post-assessment form was filled out by the participants to record their feedback after the study.

4.4   Results

Fig. 4.1 shows a typical magnitude and phase velocity plot from a transverse axial slice of the ankle. The arteries are marked and color coded. The ROI of the artery was taken per each slice to decipher a bloodflow imaging sequence.

From the bloodflow calculated over a systolic period, the flow of the three arteries can be seen in Fig. 4.2. The bloodflow shown in Fig 4.2, participant 1 shows approximately the same amount of bloodflow over the course of a systolic period. The peroneal artery shows the same peak in magnitude while the posterior and anterior tibial arteries appear to have the same flow rate. Participant 2 shows a decreased bloodflow after therapy with a decrease in the posterior and anterior tibial arteries while the peroneal artery remains roughly the same. With only two
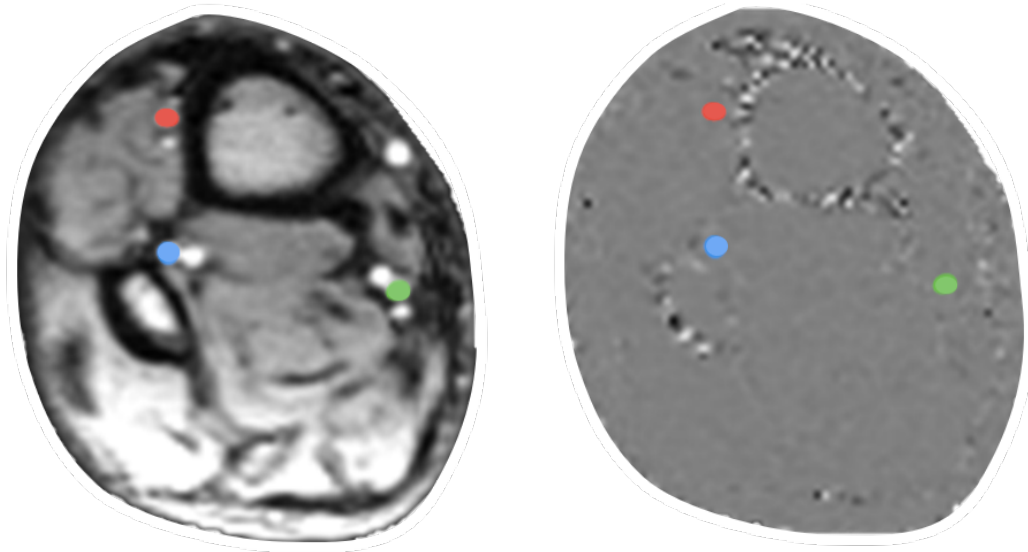
Figure 4.1: Transverse axial images of the superior ankle of participant 1 are typical for these measures. Three arteries are outlined with their respective colors labeled: anterior tibial artery (red), peroneal artery (blue), posterior tibial artery (green). The modulus image of the ankle (left) is converted to the phase velocity (right). These images are pulled from the CV Flow (Version 3.2) software.

participants, there is no statistical evidence to highlight any results, however the potential of the garment remains the same.

With the same trend as the bloodflow, participant 1 shows no change for flow velocity in Fig. 4.3. Participant 2 shows an opposite trend with an increase in velocity of the blood as it travels through the arteries. For participant 2, the posterior tibial and the peroneal arteries showed an increase in velocity while the anterior tibial artery decreased from pre-treatment to post-treatment.

4.5   Discussion

Anecdotal feedback from participant 1 and 2 reveal that the GAINS-Boot relieves pain in peripheral neuropathy. Both participants also recorded better sensation during daily activities and increased improvement in their post-therapy evaluation responses.

Participant 2 shows a decreased bloodflow with an increase in blood velocity. Potential causes include a decrease in artery cross-sectional area which would facilitate the blood to less at a faster rate. Potential factors of this vasoconstriction could potentially be from a cold pressure difference

45
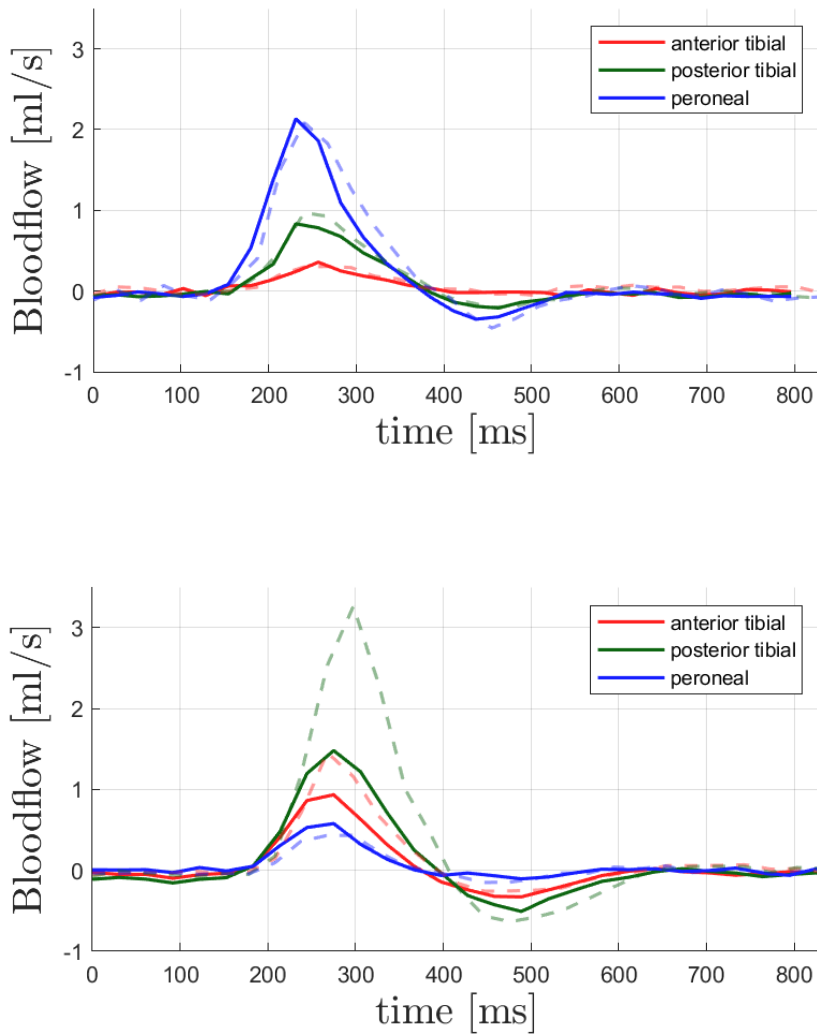
Figure 4.2: This is blood-flow data taken from participant 1 (left) and participant 2 (right) with the following key: Red - anterior tibial artery, Green - posterior tibial artery, and Blue - peroneal artery. Dashed lines are the preliminary MRI scan, with the solid lines showing the post-treatment scan.

between therapy and MRI scan. Participants were taken from the heated boot to the MRI machine. The quick temperature change from $100°$F to room temperature ($70°$F) may have causes enough of an immediate shock to create vasoconstriction and alter immediate scans [64]. Alternatively, the MRI data is limited on the length of the study and only shows data over the course of two weeks and not potential long term intervention use case results, which may provide better sensation.
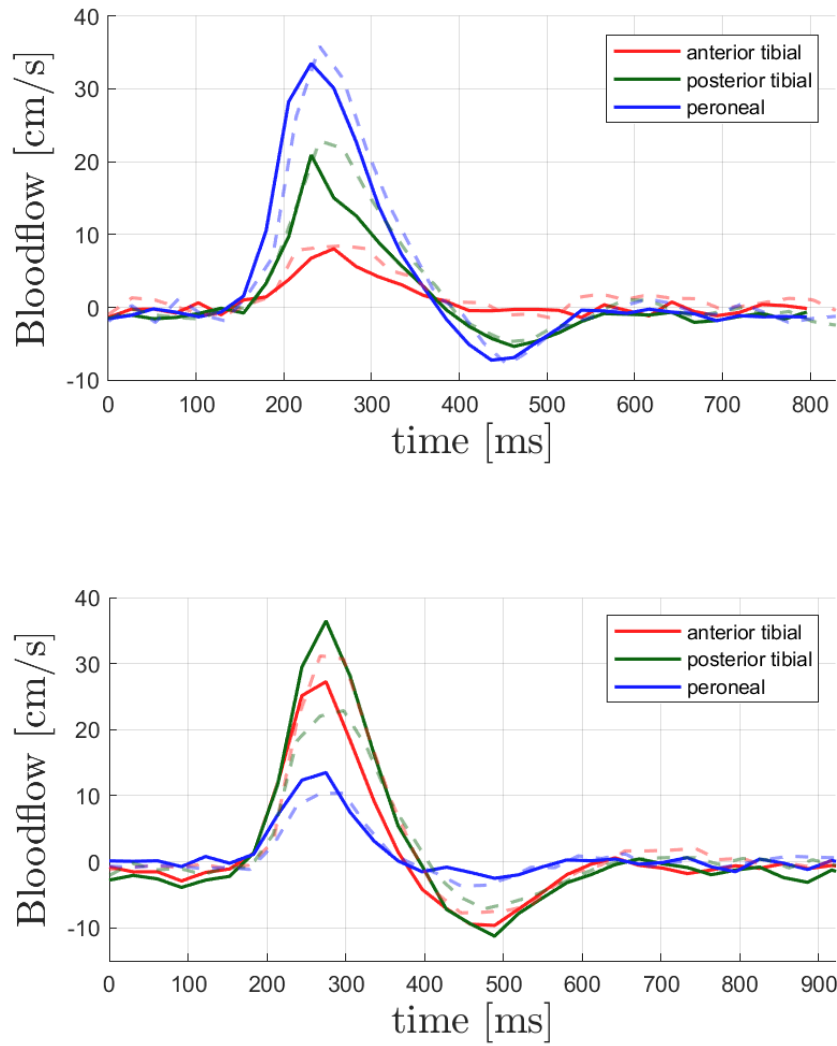
Figure 4.3: Blood velocity for participant 1 and 2 is shown in cm/s for each artery pre- and post-treatment.

Between each participant, there is a variation in different factors. Participant 2 recorded a greater pain and loss of sensation from DPN, while participant 1 recorded a much milder loss of sensation in the feet. With only two participants in this study, there is a great potential to help determine the feasibility of the therapeutic garment. With its targeted nerve focus in the distal phalanges, metatarsals, and the sural nerve, the GAINS-Boot allows for target-able and controllable vibration magnitude and frequency.

47

4.6   Future Work

The GAINS-Boot utilizes an array of heating pads controlled via a relay system within $1°$ of $100°$F. In order to increase ease of use and portability, the heated control aspect of the garment would greatly benefit from a more sophisticated, built in controller. Through the use of current control in the heating element along with a predictive model estimator, the temperature could have far less oscillation in actuality.

In future studies, measuring foot sensation via the neuropathy cartographer would provide a more clear analysis on for any improvements that the GAINS-Boot therapy may provide. Using the Semmes-Weinstein monofilament, the force of just noticeable touch can be analyzed to provide an analytical assessment. As there are only 2 diabetic participants in this study, a larger participant population would allow for a greater statistical power analysis of any overall improvement in foot sensation and overall improvement in limb pain. A clinical trial to assess the efficacy of the GAINS-Boot as a means of pain treatment assessed by the Neuropathy Cartographer in a clinical intervention study with a minimum of 16 participants (8 with non-neuropathic diabetics and 8 with neuropathic diabetics) to achieve an 80% power analysis to detect an effect size via a paired t-test.

4.7   Conclusion

To conclude, the GAINS-Boot shows promise in providing relief to peripheral neuropathy. Based on participant anecdotal feedback, the non-pharmacological interventions sessions were soothing and provided increased, lasting comfort. A non-pharmacological implementation of a rehabilitation robotic garment can provide relief and help improve QoL for participants with DPN. This intervention shows promise as a novel introduction into the field of wearable rehabilitative therapeutic robotics.

Chapter 5

Conclusion

Motor and sensory nerve rehabilitation is a growing field of research that can utilize robotic applications for rehabilitation. This thesis presents different robotic applications of motor and sensory rehabilitation.

5.1 Gravity Compensation in Upper Extremity Exoskeletons

Results from recent studies on training focused on movement quality, instead of task completion, along with the well-established role gravity compensation can play in targeting neural pathways associated with dexterous control instead of strength motivated the study in this thesis. Here, I sought to determine effects of gravity compensation on the movement quality of reaching and coordinated movement tasks. The hypothesis that these movements would show improvements in quality for both participants with chronic stroke enrolled in the study was analyzed. However, gravity compensation seemed to matter less, in particular for the less impaired participant, for the planar reaching tasks than the coordinated movements. These results, while anecdotal, motivate further study to better understand the role feedback and the focus on task completion or movement quality play on the restoration of motor function.

Post stroke rehabilitation therapy is well needed to improve gains towards a better means for quality of life. Upper-extremity rehabilitation, through the use of exoskeletons, leads this goal towards a promising outlook on post-stroke intervention. Limited by neuromuscular impairment and strength requirements, the underlying control pathways may still remain of which, gravity compensation highlights the potential for improved training in movement quality. In this thesis, I expected to see similar changes in movement quality for the reaching and coordination tasks when participants had the weight of their arm compensated by the Harmony exoskeleton. However, we

49

found differences in these movements which suggests further study for a breadth of understanding on movement quality potential and the upper echelon of improvement that can be gained through exoskeleton rehabilitation therapy.

5.2   Non-Pharmacological DPN Intervention

As diabetes rates continually increase, the need for a non-pharmacological treatment method for peripheral neuropathy rises. Harmful drugs prescribed for PPN treatment typically target the symptoms as opposed to the causation of the problem, which can lead to a numbing and resistance to pain medications. Through the use of the tri-modal stimuli provided from the GAINS-Boot, the goal of the device outlined in this thesis is to provide a therapeutic garment that can give relief to powerful, painful symptoms by encouraging the increase of vascularization, increase in cardiovascular health, and promoting neuronal stimulation.

5.3   Future Work

The Harmony Exoskeleton provides large potential in studying upper extremity movements and gravity compensation tactics. By creating a task-oriented design to therapy exercises, instead of objective oriented tasks, there may lead to an improvement in recovery potential. This can lead to a variety of separate user-feedback modalities that can allow for an individual growth response tailored to each individual.

In the future, the GAINS-Boot needs more validation with a larger population that would allow for a wider rehabilitative spectrum of participant. As a test bed, this therapeutic robotic garment may lead to implementation in other fields with minor tweaking or adjustments. I would like to see a more intricate, internal heating system that is directly apart of the garment instead of being attached on the garment as it. The control of the heat could be better implemented with a newly designed heating mesh with a heat limiter closer to the active working range of the desired temperature of the wearable device.

5.4 Conclusion

Robotics in rehabilitation can standardize intensity and dosage in novel interventions. By accounting for the amount of repetitions coupled with the time taken, these new intervention modalities provide assessment metrics alongside an increase in exercise quantities. Gravity compensation for upper extremity rehabilitation shows promising results with encouraging improvements in movement quality through the removal of strength as a necessary requirement. Controlling task feedback can allow for a higher precision in sensorimotor improvement. Other novel application of robotics give opportunity to range of neuromuscular and neural conditions. Non-pharmacological interventions through garment therapy can provide relief and help improve sensation in patients with diabetes. Overall, robotic applications in rehabilitation open up an expansive realm of possibility to help improve impairment.

Appendix A

A.1 Wiring Diagrams

Figure A.1: Temperature control PCB schematic

Figure A.2: Vibrotactile stimulation PCB schematic

A.2 Implementation Code

Listing A.1: Vibrotactile Stimulation C++ Code

```
1   #include <stdio.h>
2   #include <math.h>
3   #include <time.h>
4   #include "pico/stdlib.h"
5   #include "hardware/pwm.h"
6   #include "hardware/adc.h"
7
8   #define GPIO_ON  1
9   #define GPIO_OFF 0
10
11  int M[16] = {0, 1, 2, 3, 4, 5, 6, 7, 8, 9, 10, 11, 12, 13, 14, 15};
12
13  // Function declaration
14
15  // time conversion (t, "unit in")
16  int convT(int t, char *unit)
17  {
18      int tn;
19      if (unit == "s")
20      {
21          tn = t * 100000;
22      }
23      else if (unit == "us")
24      {
25          tn = t / 100000;
26      }
27      return tn;
28  }
29
30  // initialize pwm motors
31  void vibe(int led)
32  {
33      gpio_init(led);
34      gpio_set_function(led, GPIO_FUNC_PWM);
35  }
36
37  void h_vibe(int Mag, int freq, int M, int phi_h, int phi_v, int time, int tf)
38  {
39      // magnitude conversion
40      Mag = 53392 / 100;
41      // determine freq for slicer
42
43      for (int i = 0; i < 2; i++)
44      { // loop through row
45          ;
46      }
47  }
48
49  // main
50  int main()
```

55

```
51  {
52      // LED OUT INITIALIZATION
53      stdio_init_all();
54
55      gpio_init(LED_);
56      gpio_set_dir(LED_, GPIO_OUT);
57      gpio_put(LED_, GPIO_ON);
58
59      while (1)
60      {
61          for (int i = 0; i < 16; i++)
62          {
63              // pwm_set_gpio_level(M[i],53392);
64              gpio_init(M[i]);
65              gpio_set_dir(M[i], GPIO_OUT);
66              gpio_put(M[i], GPIO_OFF);
67          }
68          sleep_ms(1000);
69          for (int i = 0; i < 16; i++)
70          {
71              // pwm_set_gpio_level(M[i],53392);
72              gpio_init(M[i]);
73              gpio_set_dir(M[i], GPIO_OUT);
74              gpio_put(M[i], GPIO_ON);
75          }
76          sleep_ms(1000);
77      }
78  }
```

Listing A.2: Heat Control C++ Code

```
1   #include <stdio.h>
2   #include "pico/stdlib.h"
3   #include <math.h>
4   #include <time.h>
5   #include "hardware/adc.h"
6   #include "pico/binary_info.h"
7   #include "hardware/i2c.h"
8   #include "Adafruit_ADS1X15.h"
9
10  // Constants
11  float ref = 100;                    // Degrees Farenheit
12  uint64_t filt_diff = 100000;        // timer frequency between loops .1 (s) in us
13  uint64_t control_diff = 1000000;    // timer frequency between loops 1 (s) in us
14  double T = 0;
15  double R = 0;
16  double T_c = 0;                     // initializing double
17  double T_f = 0;                     // initializing double
18  double R1 = 9970;                   // 10k
19  double T0 = 298.15;                 // K
20  double B = 3950;                    // K
21  double r_inf = R1 * exp(-B / T0);   // r_inf
22
23  // BW Filter
```

```
24  float num[] = {0.0036, 0.0072, 0.0036};
25  float den[] = {1, -1.8227, 0.8372};
26
27  // Temp Control
28  float xx[][8] = {
29      {0, 0, 0},
30      {0, 0, 0},
31      {0, 0, 0},
32      {0, 0, 0},
33      {0, 0, 0},
34      {0, 0, 0},
35      {0, 0, 0},
36      {0, 0, 0}};
37
38  float yy[][8] = {
39      {0, 0, 0},
40      {0, 0, 0},
41      {0, 0, 0},
42      {0, 0, 0},
43      {0, 0, 0},
44      {0, 0, 0},
45      {0, 0, 0},
46      {0, 0, 0}};
47
48  // read locations
49  int16_t adc[] = {0, 0, 0, 0, 0, 0, 0, 0}; // read adc
50  float volts[] = {0, 0, 0, 0, 0, 0, 0, 0}; // adc -> volts
51  float err[] = {0, 0, 0, 0, 0, 0, 0, 0};    // err in system
52  int control[] = {1, 1, 1, 1, 1, 1, 1, 1}; // control out, binary
53  int last_control[] = {0, 0, 0, 0, 0, 0, 0, 0};
54  int HP_pin[] = {6, 7, 8, 9, 11, 10, 13, 12};
55  // changed to the pins used for HP control to Relay
56
57  // initialize volts to farenheit function
58  int v2f(float volt) // take in voltage
59  {
60      float R = (volt * R1) / (3.30 - volt); // resistance across the thermistor
61      float T = B / (log(R / r_inf));         // Kelvin
62      float T_c = T - 273.15;                 // convert to  C
63      float T_f = (9 * (T_c) / 5) + 32;       // convert to  F
64      return T_f;                             // return temperature in   F
65  }
66
67  int main()
68  {
69      sleep_ms(2000);
70      stdio_init_all();
71      gpio_init(25);
72      gpio_set_dir(25, GPIO_OUT);
73
74      sleep_ms(2000);
75      gpio_put(25, 1);
76
77      // Enable UART so we can print status output
```

```
78        i2c_init(i2c_default, 100 * 1000);
79        gpio_set_function(PICO_DEFAULT_I2C_SDA_PIN, GPIO_FUNC_I2C);
80        gpio_set_function(PICO_DEFAULT_I2C_SCL_PIN, GPIO_FUNC_I2C);
81        gpio_pull_up(PICO_DEFAULT_I2C_SDA_PIN);
82        gpio_pull_up(PICO_DEFAULT_I2C_SCL_PIN);
83        stdio_init_all();
84
85        Adafruit_ADS1015 ads1(0x48); // Original ADS1015 - address grounded
86        Adafruit_ADS1015 ads2(0x49); // Second ADS1015 - address -> vin
87
88        u_int64_t timer0 = time_us_64(); // current time every loop
89        u_int64_t timer1 = time_us_64(); // Filter loop
90        u_int64_t timer2 = time_us_64(); // Control loop
91
92        sleep_ms(2000);
93        gpio_put(25, 0);
94
95        while (true)
96        {
97            if ((timer0 - timer1) >= filt_diff) // Data Filter 'if' loop
98            {
99                // read voltage
100               for (int i = 0; i < 8; i++)
101               {
102
103                   // read voltage per each analog in
104                   if (i < 4)
105                   {
106                       adc[i] = ads1.readADC_SingleEnded(i);
107                       volts[i] = ads1.computeVolts(adc[i]);
108                   }
109                   // case switching for 2nd adc
110                   else
111                   {
112                       adc[i] = ads2.readADC_SingleEnded(i - 4); // i-4 for 0->3
113                       volts[i] = ads2.computeVolts(adc[i]);
114                   }
115
116                   // BW Digital Filtering
117                   xx[i][0] = v2f(volts[i]);                    // digital heat reading
118                   yy[i][0] = (num[0] * xx[i][0] + num[1] * xx[i][1]
119                   + num[2] * xx[i][2] - den[1] * yy[i][1] - den[2] *
120                   yy[i][2]); // 2nd order BW w/ cutoff at 4Hz
121                   xx[i][2] = xx[i][1];                         // if 2nd order
122                   yy[i][2] = yy[i][1];                         // if 2nd order
123                   xx[i][1] = xx[i][0];
124                   yy[i][1] = yy[i][0];                         // filtered heat reading
125
126                   err[i] = ref - yy[i][0];
127               }
128               timer1 = time_us_64(); // restate control timer
129           }
130           if ((timer0 - timer2) >= control_diff) // Control 'if' control loop
131           {
```

```
132                printf("%i,", 0);
133                for (int i = 0; i < 8; i++)
134                {
135                    last_control[i] = control[i];
136                    if (err[i] < -10)
137                    { // if anye one too hot
138                        printf("TooHot,");
139                        for (int j = 0; j < 8; j++)
140                        {
141                            last_control[j] = 0; // set switch to off (NC position)
142                            gpio_init(HP_pin[i]);
143                            gpio_set_dir(HP_pin[i], GPIO_OUT);
144                            gpio_put(HP_pin[i], last_control[i]);
145                            printf("%4.21f, %i, ", yy[j][0], last_control[j]);
146                            // print for logging
147                        }
148
149                        printf("\n");
150                        break;
151                    }
152                    else
153                    {
154                        if (err[i] > 0.5)
155                        {                    // If HP < 99.5; turn on
156                            last_control[i] = 1; // 0
157                        }
158                        else if (err[i] < -.5)
159                        {                    // if HP > 100.0 turn off
160                            last_control[i] = 0; // 1;
161                        }
162                    }
163
164                    // Data logging every control loop
165                    gpio_init(HP_pin[i]);
166                    gpio_set_dir(HP_pin[i], GPIO_OUT);
167                    gpio_put(HP_pin[i], last_control[i]);              // set relays
168                    printf("%4.21f, %i, ", yy[i][0], last_control[i]); // print for logging
169                }
170
171            printf("\n");
172            timer2 = time_us_64(); // restate control timer
173            }
174        timer0 = time_us_64(); // restate "true" timer
175    }
176 }
```

Listing A.3: Pressure Monitoring python Code

```
1 import rclpy
2 from rclpy.node import Node
3 from std_msgs.msg import Float64
4
5 # Pressure adds
6 import board
```

```
 7  import adafruit_mprls
 8  import adafruit_tca9548a
 9
10  class MinimalPublisher(Node):
11
12
13
14      def __init__(self):
15          super().__init__('Pressure_Publisher')
16
17          # initialize pressure
18          i2c = board.I2C()   # uses board.SCL and board.SDA
19          self.tca = adafruit_tca9548a.TCA9548A(i2c)
20          self.mpr1 = adafruit_mprls.MPRLS(self.tca[0], psi_min=0, psi_max=25)
21          self.mpr2 = adafruit_mprls.MPRLS(self.tca[1], psi_min=0, psi_max=25)
22          self.mpr3 = adafruit_mprls.MPRLS(self.tca[2], psi_min=0, psi_max=25)
23          self.mpr4 = adafruit_mprls.MPRLS(self.tca[3], psi_min=0, psi_max=25)
24
25          self.publisher1_ = self.create_publisher(Float64, 'pressure1', 10)
26          self.publisher2_ = self.create_publisher(Float64, 'pressure2', 10)
27              self.publisher3_ = self.create_publisher(Float64, 'pressure3', 10)
28          self.publisher4_ = self.create_publisher(Float64, 'pressure4', 10)
29          timer_period = 0.1   # seconds
30          self.timer = self.create_timer(timer_period, self.timer_callback)
31          self.i = 0
32
33      ## Put the callback
34      def timer_callback(self):
35          msg1 = Float64()
36          msg2 = Float64()
37          msg3 = Float64()
38          msg4 = Float64()
39
40          msg1.data = self.mpr1.pressure
41          msg2.data = self.mpr2.pressure
42          msg3.data = self.mpr3.pressure
43          msg4.data = self.mpr4.pressure
44          self.publisher1_.publish(msg1)
45          self.publisher2_.publish(msg2)
46          self.publisher3_.publish(msg3)
47          self.publisher4_.publish(msg4)
48          self.i += 1
49
50  def main(args=None):
51      rclpy.init(args=args)
52
53      minimal_publisher = MinimalPublisher()
54
55      rclpy.spin(minimal_publisher)
56
57      # Destroy the node explicitly
58      minimal_publisher.destroy_node()
59      rclpy.shutdown()
60
```

```
61
62 if __name__ == '__main__':
63     main()
```

Bibliography

[1] R. O. Hailey, A. C. De Oliveira, K. Ghonasgi, B. Whitford, R. K. Lee, C. G. Rose, and A. D. Deshpande, "Impact of Gravity Compensation on Upper Extremity Movements in Harmony Exoskeleton," in *IEEE International Conference on Rehabilitation Robotics*, vol. 2022-July. IEEE Computer Society, 2022.

[2] A. H. A. Stienen, E. E. G. Hekman, F. C. T. Van Der Helm, G. B. Prange, M. J. A. Jannink, A. M. M. Aalsma, and H. Van Der Kooij, "Freebal: dedicated gravity compensation for the upper extremities," in *International Conference on Rehabilitation Robotics (ICORR)*, 2007, pp. 804–808.

[3] R. J. Sanchez, J. Liu, S. Rao, P. Shah, R. Smith, T. Rahman, S. C. Cramer, J. E. Bobrow, and D. J. Reinkensmeyer, "Automating arm movement training following severe stroke: Functional exercises with quantitative feedback in a gravity-reduced environment," *IEEE Transactions on Neural Systems and Rehabilitation Engineering*, vol. 14, no. 3, pp. 378–389, 9 2006.

[4] Hocoma, "Armeo Spring." [Online]. Available: https://www.hocoma.com/us/solutions/armeo-spring/

[5] C. Vitale Kyle, J. Robert L, and Z. Michael E, "Contact Mechanics Modeling of the Semmes-Weinstein Monofilament on the Plantar Surface of the Foot," *International Journal of Foot and Ankle*, vol. 5, no. 2, 5 2021.

[6] "Normatec." [Online]. Available: https://hyperice.com/products/normatec-3-legs/

[7] CDC, "Stroke Facts." [Online]. Available: https://www.cdc.gov/stroke/facts.html

[8] R. Gassert and V. Dietz, "Rehabilitation robots for the treatment of sensorimotor deficits: A neurophysiological perspective," *Journal of NeuroEngineering and Rehabilitation*, vol. 15, no. 1, pp. 1–15, 6 2018.

[9] NIH, "Stroke." [Online]. Available: https://www.ninds.nih.gov/post-stroke-rehabilitation-fact-sheet

[10] C. M. Stinear, W. D. Byblow, S. J. Ackerley, M. C. Smith, V. M. Borges, and P. A. Barber, "Proportional Motor Recovery after Stroke: Implications for Trial Design," *Stroke*, vol. 48, no. 3, pp. 795–798, 3 2017.

[11] "Diabetes," 2023. [Online]. Available: https://www.niddk.nih.gov/health-information/diabetes

[12] T. Gordon, "Peripheral nerve regeneration and muscle reinnervation," *International Journal of Molecular Sciences*, vol. 21, no. 22, pp. 1–24, 11 2020.

[13] Y. Hara, "Brain Plasticity and Rehabilitation in Stroke Patients," *J Nippon Med Sch*, vol. 82, no. 1, 2015. [Online]. Available: www.nms.ac.jp!

[14] S. K. Lee and S. W. Wolfe, MD, "Peripheral Nerve Injury and Repair," *Journal of the American Academy of Orthopaedic Surgeons*, vol. 8, no. 4, pp. 243–252, 8 2000.

[15] M. Modrak, M. A. Talukder, K. Gurgenashvili, M. Noble, and J. C. Elfar, "Peripheral nerve injury and myelination: Potential therapeutic strategies," *Journal of Neuroscience Research*, vol. 98, no. 5, pp. 780–795, 5 2020.

[16] C. Jh and S. Rb, "THE CHANGING FACE OF NEUROLOGICAL REHABILITATION," *Rev. bras. fisioter*, vol. 10, no. 2, pp. 147–156, 2006.

[17] V. S. Huang and J. W. Krakauer, "Robotic neurorehabilitation: A computational motor learning perspective," *Journal of NeuroEngineering and Rehabilitation*, vol. 6, no. 1, 2009.

[18] V. R. Edgerton, N. J. Tillakaratne, A. J. Bigbee, R. D. De Leon, and R. R. Roy, "Plasticity of the spinal neural circuitry after injury," *Annual Review of Neuroscience*, vol. 27, pp. 145–167, 2004.

[19] C. G. Rose, A. D. Deshpande, J. Carducci, and J. D. Brown, "The road forward for upper-extremity rehabilitation robotics," 9 2021.

[20] N. Hogan, "Impedance control: An approach to manipulation: Part II–Implmentation," *Journal of Dynamic Systems*, vol. 107, no. 9, pp. 8–16, 3 1985. [Online]. Available: http://asmedigitalcollection.asme.org/dynamicsystems/article-pdf/107/1/8/5492420/8_1.pdf

[21] H. Igo Krebs, N. Hogan, M. L. Aisen, and B. T. Volpe, "Robot-aided neurorehabilitation," *IEEE Transactions on Rehabilitation Engineering*, vol. 6, no. 1, pp. 75–87, 1998. [Online]. Available: https://pubmed.ncbi.nlm.nih.gov/9535526/

[22] L. M. Weber and J. Stein, "The use of robots in stroke rehabilitation: A narrative review," *NeuroRehabilitation*, vol. 43, no. 1, pp. 99–110, 2018.

[23] G. Mochizuki, A. Centen, M. Resnick, C. Lowrey, S. P. Dukelow, and S. H. Scott, "Movement kinematics and proprioception in post-stroke spasticity: Assessment using the Kinarm robotic exoskeleton," *Journal of NeuroEngineering and Rehabilitation*, vol. 16, no. 1, 11 2019.

[24] A. Jayatilaka, N. Alyousef, J. Doyle, H. Kachhvi, G. Parsons, F. Ismail, C. Boulias, S. Reid, C. Phadke, K. Hreha, I. Hong, M. Pappadis, C.-Y. Li, R. Deer, J. Dean, A. Na, S. Nowakowski, S. Bhavnani, H. Shaltoni, and T. Reistetter, "Upper Limb Spasticity Measurement From Manual Assessment of Dynamic Stretch Reflex Threshold Using a Metronome Using Visual Analytics to Inform a Stroke Specific Self-Management Program," Tech. Rep. [Online]. Available: www.archives-pmr.org

[25] D. Gijbels, I. Lamers, L. Kerkhofs, G. Alders, E. Knippenberg, and P. Feys, "The Armeo Spring as training tool to improve upper limb functionality in multiple sclerosis: A pilot study," *Journal of NeuroEngineering and Rehabilitation*, vol. 8, no. 1, 2011.

[26] L. Oujamaa, I. Relave, J. Froger, D. Mottet, and J. Y. Pelissier, "Rehabilitation of arm function after stroke. Literature review," *Annals of Physical and Rehabilitation Medicine*, vol. 52, no. 3, pp. 269–293, 4 2009.

[27] B. Kim and A. D. Deshpande, "An upper-body rehabilitation exoskeleton Harmony with an anatomical shoulder mechanism: Design, modeling, control, and performance evaluation," *International Journal of Robotics Research*, vol. 36, no. 4, pp. 414–435, 4 2017.

[28] B. Kim and A. Deshpande, "Controls for the shoulder mechanism of an upper-body exoskeleton for promoting scapulohumeral rhythm," in *International Conference of Rehabilitation Robotics (ICORR)*. IEEE, 2015.

[29] V. Arakelian, "Gravity compensation in robotics," *Advanced Robotics*, vol. 30, no. 2, pp. 79–96, 1 2016.

[30] N. Hogan, H. I. Krebs, J. Charnnarong, P. Srikrishna, and A. Sharon, "MIT - MANUS: A workstation for manual therapy and training I," in *1992 Proceedings IEEE International Workshop on Robot and Human Communication, ROMAN 1992*. IEEE, 1992, pp. 161–165.

[31] Mayo Clinic, "Peripheral Neuropathy." [Online]. Available: https://www.mayoclinic.org/diseases-conditions/peripheral-neuropathy/symptoms-causes/syc-20352061

[32] V. Baute, D. Zelnik, J. Curtis, and F. Sadeghifar, "Complementary and Alternative Medicine for Painful Peripheral Neuropathy," *Current Treatment Options in Neurology*, vol. 21, no. 9, 9 2019.

[33] K. Barrell and A. G. Smith, "Peripheral Neuropathy," *Medical Clinics of North America*, vol. 103, no. 2, pp. 383–397, 3 2019.

[34] S. S. Virani, A. Alonso, E. J. Benjamin, M. S. Bittencourt, C. W. Callaway, A. P. Carson, A. M. Chamberlain, A. R. Chang, S. Cheng, F. N. Delling, L. Djousse, M. S. Elkind, J. F. Ferguson, M. Fornage, S. S. Khan, B. M. Kissela, K. L. Knutson, T. W. Kwan, D. T. Lackland, T. T. Lewis, J. H. Lichtman, C. T. Longenecker, M. S. Loop, P. L. Lutsey, S. S. Martin, K. Matsushita, A. E. Moran, M. E. Mussolino, A. M. Perak, W. D. Rosamond, G. A. Roth, U. K. Sampson, G. M. Satou, E. B. Schroeder, S. H. Shah, C. M. Shay, N. L. Spartano, A. Stokes, D. L. Tirschwell, L. B. VanWagner, C. W. Tsao, S. S. Wong, and D. G. Heard, "Heart disease and stroke statistics 2020 update: A report from the American Heart Association," pp. E139–E596, 2020.

[35] N. Schweighofer, C. Wang, D. Mottet, I. Laffont, K. Bakthi, D. J. Reinkensmeyer, and O. Rémy-Néris, "Dissociating motor learning from recovery in exoskeleton training post-stroke," *Journal of NeuroEngineering and Rehabilitation*, vol. 15, no. 1, 10 2018.

[36] J. W. Krakauer, T. Kitago, J. Goldsmith, O. Ahmad, P. Roy, J. Stein, L. Bishop, K. Casey, B. Valladares, M. D. Harran, J. C. Cortés, A. Forrence, J. Xu, S. DeLuzio, J. P. Held, A. Schwarz, L. Steiner, M. Widmer, K. Jordan, D. Ludwig, M. Moore, M. Barbera, I. Vora, R. Stockley, P. Celnik, S. Zeiler, M. Branscheidt, G. Kwakkel, and A. R. Luft, "Comparing a Novel Neuroanimation Experience to Conventional Therapy for High-Dose Intensive Upper-Limb Training in Subacute Stroke: The SMARTS2 Randomized Trial," *Neurorehabilitation and Neural Repair*, vol. 35, no. 5, pp. 393–405, 5 2021.

[37] M. D. Ellis, T. Sukal-Moulton, and J. P. Dewald, "Progressive shoulder abduction loading is a crucial element of arm rehabilitation in chronic stroke," *Neurorehabilitation and Neural Repair*, vol. 23, no. 8, pp. 862–869, 10 2009.

[38] M. R. Senesh, K. Barragan, and D. J. Reinkensmeyer, "Rudimentary Dexterity Corresponds With Reduced Ability to Move in Synergy After Stroke: Evidence of Competition Between Corticoreticulospinal and Corticospinal Tracts?" *Neurorehabilitation and Neural Repair*, vol. 34, no. 10, pp. 904–914, 10 2020.

[39] A. C. d. Oliveira, C. G. Rose, K. Warburton, E. M. Ogden, B. Whitford, R. K. Lee, and A. D. Deshpande, "Exploring the Capabilities of Harmony for Upper-Limb Stroke Therapy," in *IEEE International Conference of Rehabilitation Robotics (ICORR)*. Toronto, Canada: IEEE ICORR, 6 2019.

[40] R. F. Beer, C. Naujokas, B. Bachrach, and D. Mayhew, "Development and evaluation of a gravity compensated training environment for robotic rehabilitation of post-stroke reaching," in *Conference on Biomedical Robotics and Biomechatronics*. IEEE, 2008, pp. 205–210.

[41] N. Nordin, S. Quan Xie, and B. Wünsche, "Assessment of movement quality in robot-assisted upper limb rehabilitation after stroke: a review," *Journal of NeuroEngineering and Rehabilitation*, vol. 11, p. 137, 2014. [Online]. Available: http://www.jneuroengrehab.com/content/11/1/137

[42] H. I. Krebs, B. T. Volpe, D. Williams, J. Celestino, S. K. Charles, D. Lynch, and N. Hogan, "Robot-aided neurorehabilitation: A robot for wrist rehabilitation," *IEEE Transactions on Neural Systems and Rehabilitation Engineering*, vol. 15, no. 3, pp. 327–335, 9 2007.

[43] P. Garrec, J. P. Friconneau, Y. Méasson, and Y. Perrot, "ABLE, an innovative transparent exoskeleton for the upper-limb," in *2008 IEEE/RSJ International Conference on Intelligent Robots and Systems, IROS*, 2008, pp. 1483–1488.

[44] R. L. Smith, J. Lobo-Prat, H. Van Der Kooij, and A. H. Stienen, "Design of a perfect balance system for active upper-extremity exoskeletons," in *IEEE International Conference on Rehabilitation Robotics*, 2013.

[45] A. C. De Oliveira, J. S. Sulzer, and A. D. Deshpande, "Assessment of Upper-Extremity Joint Angles Using Harmony Exoskeleton," *IEEE Transactions on Neural Systems and Rehabilitation Engineering*, vol. 29, pp. 916–925, 2021.

[46] C. G. Rose, E. Pezent, C. K. Kann, A. D. Deshpande, and M. K. O'Malley, "Assessing Wrist Movement with Robotic Devices," *IEEE Transactions on Neural Systems and Rehabilitation Engineering*, vol. 26, no. 8, pp. 1585–1595, 8 2018.

[47] Y. Meziani, Y. Morère, A. Hadj-Abdelkader, M. Benmansour, and G. Bourhis, "Towards adaptive and finer rehabilitation assessment: A learning framework for kinematic evaluation of upper limb rehabilitation on an Armeo Spring exoskeleton," *Control Engineering Practice*, vol. 111, 6 2021.

[48] S. K. Charles and N. Hogan, "The curvature and variability of wrist and arm movements," *Experimental Brain Research*, vol. 203, no. 1, pp. 63–73, 5 2010.

[49] S. Balasubramanian, A. Melendez-Calderon, A. Roby-Brami, and E. Burdet, "On the analysis of movement smoothness," *Journal of NeuroEngineering and Rehabilitation*, vol. 12, p. 112, 2015.

[50] P. d. Leva, "Adjustments to Zatsiorsky-Seluyanov's segment inertia parameters," *Journal of Biomechanics*, vol. 29, no. 9, pp. 1223–1230, 1996. [Online]. Available: https://doi.org/10.1016/0021-9290(95)00178-6

[51] N. Jarrassé and G. Morel, "Connecting a human limb to an exoskeleton," *IEEE Transactions on Robotics*, vol. 28, no. 3, pp. 697–709, 2012.

[52] J. W. Krakauer, T. Kitago, J. Goldsmith, O. Ahmad, P. Roy, J. Stein, L. Bishop, K. Casey, B. Valladares, M. D. Harran, J. C. Cortés, A. Forrence, J. Xu, S. DeLuzio, J. P. Held, A. Schwarz, L. Steiner, M. Widmer, K. Jordan, D. Ludwig, M. Moore, M. Barbera, I. Vora, R. Stockley, P. Celnik, S. Zeiler, M. Branscheidt, G. Kwakkel, and A. R. Luft, "Comparing a Novel Neuroanimation Experience to Conventional Therapy for High-Dose Intensive Upper-Limb Training in Subacute Stroke: The SMARTS2 Randomized Trial," *Neurorehabilitation and Neural Repair*, vol. 35, no. 5, pp. 393–405, 5 2021.

[53] S. McDevitt, H. Hernandez, J. Hicks, R. Lowell, H. Bentahaikt, R. Burch, J. Ball, H. Chander, C. Freeman, C. Taylor, and B. Anderson, "Wearables for Biomechanical Performance Optimization and Risk Assessment in Industrial and Sports Applications," *Bioengineering*, vol. 9, no. 1, 1 2022.

[54] "Aquilo Cold-Compression Boots." [Online]. Available: https://aquilosports.com/products/aquilo-cryocompression-boots?variant=40065226539142

[55] "Rapid Reboot." [Online]. Available: https://rapidreboot.com/

[56] V. E. Brunt and C. T. Minson, "Heat therapy: mechanistic underpinnings and applications to cardiovascular health," *Journal of Applied Physiology*, pp. 1684–1704, 2021. [Online]. Available: http://www.jap.org

[57] T. Urbanek, M. Juśko, W. B. Kuczmik, and M. Jusko, "Compression therapy for leg oedema in patients with heart failure," *ESC Heart Failure*, 2020. [Online]. Available: https://onlinelibrary.wiley.com/doi/10.1002/ehf2.12848

[58] K. Pawlaczyk, M. Gabriel, T. Urbanek, . Dzieciuchowicz, Z. Krasiński, Z. Gabriel, M. N. Olejniczak, and M. Stanisić, "Effects of intermittent pneumatic compression on reduction of postoperative lower extremity edema and normalization of foot microcirculation flow in patients undergoing arterial revascularization," *Medical Science Monitor*, vol. 21, pp. 3986–3992, 12 2015.

[59] Y. Takatsuru, D. Fukumoto, M. Yoshitomo, T. Nemoto, H. Tsukada, and J. Nabekura, "Neuronal circuit remodeling in the contralateral cortical hemisphere during functional recovery from cerebral infarction," *Journal of Neuroscience*, vol. 29, no. 32, pp. 10 081–10 086, 8 2009.

[60] J. Hong, M. Barnes, and N. Kessler, "Case study: Use of vibration therapy in the treatment of diabetic peripheral small fiber neuropathy," *Journal of Bodywork and Movement Therapies*, vol. 17, no. 2, pp. 235–238, 4 2013.

[61] V. K. Castellano, "Design, Performance, and Analysis of an Automated Tool for Neuropathy Assessment on the Plantar Surface," Ph.D. dissertation, Auburn University, Auburn, 8 2022.

[62] "Sunbeam Heating Pad." [Online]. Available: https://www.sunbeam.com/pain-relief/general-muscle-pain/standard-size-heating-pad/SAP_2101860.html

[63] H. M. Nagaraj, A. Pednekar, C. Corros, H. Gupta, and S. G. Lloyd, "Determining Exercise-Induced Blood Flow Reserve in Lower Extremities Using Phase Contrast MRI," *J. Magn. Reson. Imaging*, vol. 27, pp. 1096–1102, 2008. [Online]. Available: https://onlinelibrary.wiley.com/doi/10.1002/jmri.21336

[64] J. R. House, A. E. Michael, and J. Tipton, "Using skin temperature gradients or skin heat flux measurements to determine thresholds of vasoconstriction and vasodilatation," *European Journal of Applied Physiology*, 2002.